VOLUME 18, 1956/57, No. 3 pp. 73-100 Published 14th September 1956

Philips Technical Review

DEALING WITH TECHNICAL PROBLEMS
RELATING TO THE PRODUCTS, PROCESSES AND INVESTIGATIONS OF
THE PHILIPS INDUSTRIES

EDITED BY THE RESEARCH LABORATORY OF N.V. PHILIPS' GLOEILAMPENFABRIEKEN, EINDHOVEN, NETHERLANDS

# A PENTODE GUN FOR TELEVISION PICTURE TUBES

by J. C. FRANCKEN, J. de GIER and W. F. NIENHUIS.

621.385.832.032.269.1:621.397.62

*As a result of improvements in the quality of the transmitted television picture, higher demands are being made on picture tubes. The characteristics of the electron gun play a fundamental part in this respect. Owing to the use of different line systems in different countries, it can be desirable, as this article will show, to have a gun that is also capable of variation. With the "pentode" gun described here the optimum quality can be simply adjusted for any line system.*

The function of the electron gun in a television picture tube is to form a beam of electrons. By means of an electron lens, the electron beam is then focussed upon the fluoresecnt screen where it appears as a spot of light. The spot of light scans a frame the brightness of which must vary synchronously point by point with the intensity of the received television signal. For this purpose the electron gun is provided with a control grid, which controls the current of the electron beam as a function of the signal voltage.

The simplest type of electron gun (see *fig. 1*) consists of three electrodes (triode gun): the cathode ($k$), the control grid ($g_1$) and a second electrode ($g_2$) usually called the anode, which gives the electrons the energy needed to produce a bright picture. The electric field between $g_2$ and $g_1$ functions as a positive lens and thus makes the beam less divergent.

The characteristics of a triode gun are closely related to those of a triode valve. For example, in a triode gun the current $I_s$ flowing to the anode — and through the anode to the screen — is highly dependent upon the anode voltage $V_{g2}$. At moderate currents, the brillance of the image on the screen is proportional to the product $I_s V_{g2}$. As a result, the brilliance varies more than proportionally to $V_{g2}$. This is usually undesirable, in view of the difficulty and expense involved in adequately stabilizing the anode voltage $V_{g2}$, which may be between 12 and 16 kV in modern tubes.

For this reason the electron gun most commonly used is the tetrode type as sketched in *fig. 2*. The anode in this gun consists of two parts: the first and final anodes $g_2$ and $g_3$. The first anode carries a potential of 300 V and is so designed that hardly any electrons fall on it. There is no difficulty in stabilizing this voltage. The beam current $I_s$ is determined almost entirely by $V_{g1}$ and $V_{g2}$, and is practically unaffected by the high potential $V_{g3}$ on the final anode. The brilliance is now only

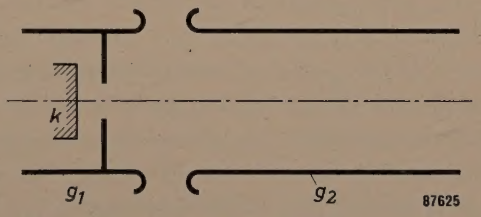

Fig. 1. The simplest form of electron gun (triode gun). $k$ cathode, $g_1$ control grid, $g_2$ anode.

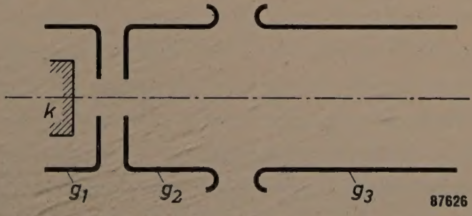

Fig. 2. Tetrode gun. $k$ cathode, $g_1$ control grid, $g_2$ first anode, $g_3$ final anode.

*proportional* to the final anode voltage (here $V_{g3}$), so that this voltage need no longer be so accurately stabilized. Another important advantage of the tetrode gun is that, owing to the lens action of the field between $g_2$ and $g_3$, the emergent beam is more convergent than is the case on a triode (more prefocussing). Moreover, the extra parameter allows more latitude in selecting the degree of prefocussing required. As will be shown, this characteristic has an important bearing on the quality of the picture.

*Fig. 3* represents schematically the complete electrode system of a picture tube, showing the path of the electrons. One may regard the system as consisting of four components: the gun with electrodes $k$, $g_1$, $g_2$ and $g_3$, the focussing lens $f$, the deflection coils $D$ and the screen $s$. Excluding the action of the lens f, the electron gun prefocusses the beam to produce a spot of light of diameter $d_V$ on the screen. If the lens $f$ is now introduced, the beam is focussed sharply, resulting in a smaller spot of diameter $d_s$. The width of the beam in the deflection coils is then $d_D$. By means of the magnetic field of the coils D, the spot can be made to scan the screen to produce a television frame.

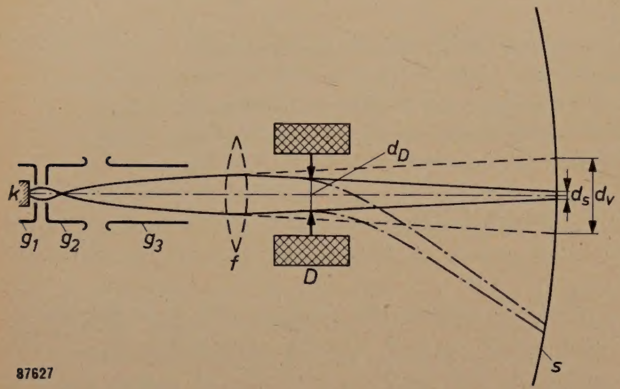

Fig. 3. The electrodes of a picture tube and the path of the electron beam. $K$, $g_1$, $g_2$ and $g_3$ together constitute the tetrode gun. D deflection coils, $s$ screen, $d_V$ and $d_s$ diameters of focussed and unfocussed spots respectively, $d_D$ beam width of focussed beam in the deflection coils.

It has been found in practice that more parameters are needed for adjusting the electron gun, especially if one and the same type of tube is to be used for all the different line scans of European television transmissions. We have therefore designed an electron gun with five electrodes and this pentode gun is now being used in nearly all Philips picture tubes. We shall be better able to discuss the possibilities of the pentode gun by first considering some general matters of design and electron optics. Finally, we shall describe in more detail the practical construction of the gun.

## The requirements to be met by the gun and the picture formation

The first requirement is a picture of adequate brightness. As stated, at moderate currents the brilliance with a given screen material is proportional to the power of the beam. This more or less fixes the requisite value of the product $I_s V_{g3}$. Further, the spot on the screen should be so small as to allow the sharpness of the picture to be determined exclusively by the television system, i.e. by the number of lines per frame and the bandwidth. This is the case if the lines of the frame can only just be separately distinguished on the tube srceen. The spot becomes smaller as $V_{g3}$ increases and $I_s$ decreases. If the price is to be kept down, both values will be separately fixed by these factors. Moreover, the spot should only be slightly larger in the corners of the screen than in the centre. Since modern tubes are required to be short in order to keep the size of the television cabinet within manageable proportions, the gun itself must be short and larger angles of deflection must be used [1]).

Now, spot size increases with the deflection angle. This deflection-defocussing has two causes:

1) The curvature of the focal plane is greater than that of the picture tube screen. If the middle of the picture is well focussed, the focus at the edges lies behind the screen (i.e. inside the tube).
2) An increasing angle of deflection causes increasing astigmatism. The magnitude of this aberration depends upon the design of the deflection coils.

Both defocussing effects are reduced the smaller the diameter of the beam where it passes between the deflection coils. There is therefore a prescribed maximum for the diameter $d_D$ in fig. 3: the beam must not exceed a certain specified width, and this is largely determined by the degree of prefocussing and the position of the focussing lens. The question now is what means should be adopted to obtain a narrow beam and what is the optimum that can be achieved.

## Electron-optical considerations

### *The Abbe sine condition*

The Abbe sine condition states that if a small plane object of area $S$, situated in a region of refractive index $n$ forms an image of area $S'$ in a region of refractive index $n'$, the semi-angles of the cones of the emergent and incident rays being $u$ and $u'$ respectively (see *fig. 4*).

---

[1]) For a more detailed treatment see J. L. H. Jonker, Philips tech. Rev. 14, 361-367, 1952/53.

$$n^2 S \sin^2 u = n'^2 S' \sin^2 u' \quad . \; . \; . \; . \; . \quad (1)$$

A similar postulate applies in electron optics. In the case of electron lenses, the potential $\Phi$ is substituted for the square of the refractive index, thus:

$$\Phi\, S \sin^2 u = \Phi'\, S' \sin^2 u' \quad . \; . \; . \; . \quad (1a)$$

(the quantities corresponding to the image are again designated by dashes). The potential is determined with respect to the plane where the electron velocity is zero, i.e. near the plane of the cathode.

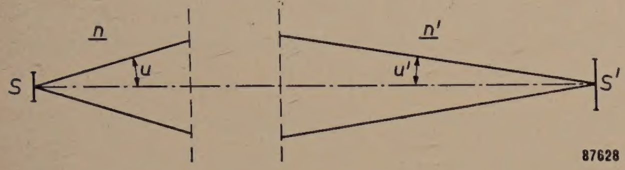

Fig. 4. Diagram to illustrate the Abbe sine condition.

By analogy with optics, we can introduce the quantity "electron-optical brightness" $B$, substituting the total beam current $I_s$ for the luminous flux. We can formulate this brightness as:

$$B = \frac{I_s}{\pi S \sin^2 u}\,.$$

If we compare the brightness $B'$ in the image space with the brightness $B$ in the object space, we see from (1a) that:

$$\frac{B'}{\Phi'} = \frac{B}{\Phi}\,.$$

The brightness can therefore be increased by raising the voltage.

In order to be able to apply (1a) to a picture tube, we must know what is acting as the object in the tube and what are its potential and its diameter.

### *Characteristics of the cross-over*

The focus of the electron beam is an image (brought about by the focussing and prefocussing lenses) of a point of intersection in the beam; this we shall call the (first) cross-over. It is formed in the triode section of the electron gun, and we shall therefore consider this section separately.

The paths of a number of electrons in the triode section are represented schematically in *fig. 5*. Each point of the cathode emits electrons in all forward directions, so that each point can be said to emit a separate beam. These beams are bent by the electric field and made to converge. The axis of an individual beam is called the principal ray; at some point along this the rays of the beam converge. This point is the image of the corresponding point on the cathode, and we therefore obtain the image $k'$ of the cathode $k$.

Between $k$ and $k'$ the principal rays intersect the axis at the position marked $C$ in fig. 5. This is the cross-over. We see that the cross-section of the total beam emitted by $k$ is smallest at this position, being almost equal to the vertical cross-section of a beam originating from a single point of $k$. The image of the cross-over appears on the screen, and it is to this image that we apply the Abbe sine condition (see 1a). All quantities referring to the cross-over are suffixed c, and those referring to the screen image are suffixed s. Furthermore, the sine is replaced by the angle itself; this is justified by the small beam angles in these tubes (paraxial approximation). The formula now becomes:

$$S_s \Phi_s u_s^2 = S_c \Phi_c u_c^2. \quad . \; . \; . \; . \quad (2)$$

Finally, we introduce a quantity $K$, defined by

$$\frac{1}{K} = S_c \Phi_c u_c^2. \quad . \; . \; . \; . \quad (3)$$

We may therefore write

$$S_s u_s^2 = \frac{1}{\Phi_s K}\,,$$

or, because $S_s = \frac{1}{4}\pi d_s^2$:

$$u_s d_s = \sqrt{\frac{4}{\pi \Phi_s K}}\,. \quad . \; . \; . \; . \; . \quad (4)$$

As we have seen, the screen potential $\Phi_s$ is predetermined ($\Phi_s = V_{g3}$). If we consider $K$ as given, the product $u_s d_s$ is also determined.

The diameter of the spot $d_s$ should, as stated, be sufficiently small. On the other hand, this should not give rise to too much deflection defocussing which, for a given size of tube, increases with increasing beam angle $u_s$, i.e. is greater the wider the beam. Since, according to (4), the product $u_s d_s$ is fixed, we must strike a compromise here. Only by increasing the value of $K$ can we reduce both the

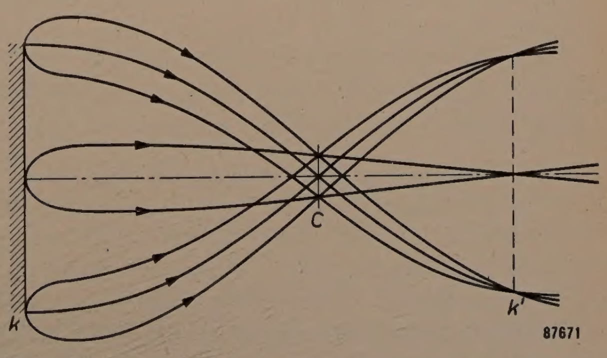

Fig. 5. The electrons from cathode $k$ form an image of the cathode at $k'$. Owing to emission in all directions, each point of $k$ emits a beam of finite width. The axes of these beams intersect at $C$, at which position the total beam is narrowest in diameter. This point is called the cross-over.

diameter of the spot and the deflection defocussing. The actual manner in which the picture is produced, for example by the number of lenses and their focal length, has no effect.

What is important, however, is that equation (4) is valid only for a perfect image. Owing to geometrical errors in the lenses (spherical aberration and axial astigmatism) and to space-charge effects, the product $u_s d_s$ is always larger than would follow from (4). (This will be dealt with in more detail under the next heading.) Formula (4) cannot therefore be used for quantitative calculations but it does serve as an indication of how the different quatities influence the solution of the problem and as a means of calculating a lower limit of the $u_s d_s$ product.

The value of $K$ is solely dependent upon the characteristics of the cross-over (see (3) ) and can in principle be derived from calculations of electron paths in the triode section. The calculation is greatly complicated by the fact that space charge effects cannot be reglected. However, by introducing certain idealisations, we can nevertheless make certain statements about $K$.

If there is uniform emission over the whole surface of the cathode and if the emitted electrons have a Maxwellian velocity distribution, the maximum current density in the cross-over (by paraxial approximation) will be, as shown by Langmuir [2]):

$$j_{c\,\max} = j_0 \left(\frac{e\Phi_c}{kT} + 1\right) \sin^2 u_c ,$$

where $j_0$ is the current density at the cathode, $T$ the absolute cathode temperature, $e$ the charge on the electron and $k$ the Boltzmann constant. If, as is usual with these tubes, $e\Phi_c \gg kT$ ($kT/e \approx 0.1$ V for $T = 1100$ °K) and $u_c \ll 1$, we can write:

$$j_{c\,\max} = \frac{e\Phi_c}{kT}\, j_0\, u_c^2 . \quad \ldots . \quad (5)$$

Assuming uniform current density in cross-over, the total current will be $I_s = j_c S_c$, and it therefore follows from (3) and (5) that:

$$K = \frac{e}{kT}\frac{j_0}{I_s} = \frac{e}{kT}\frac{1}{S_0} . \quad \ldots . \quad (6)$$

where $S_0$ is the effective cathode surface.

However, the current density in the cross-over is not uniform. From fig. 5 we see that the principal rays converge in the middle of the cross-over. The peripheral parts of the cross-over are formed by electrons emitted with lateral velocities. Starting from this premise, Dosse [3]) calculated that the average current density of the cross-over as well as $K$ are smaller by a factor of 3 than as indicated by (6).

A second correction is needed to allow for the limitation of the emission by the space charge. Owing to the space charge, the emission from the edge of the cathode is lower than in the middle. Using a simplified theory, Ploke [4]) estimated that the total cathode current is smaller by a factor of 2.5 than it would be if there were uniform emission from the whole cathode surface. Taking $j_0'$ to be the current density in the middle,

$$I_s = 0{\cdot}4\, S_0 j_0' .$$

Since all points of the cathode contribute to the density of each point in the cross-over (see fig. 5) this density too is reduced by a factor of 2.5.

Owing to both causes, $K$ is finally found to be:

$$K = \frac{1}{7.5}\frac{j_0'}{I_s}\frac{e}{kT} . \quad \ldots\ldots \quad (7)$$

The value of $I_s$ being predetermined (see above) it follows from these formulae that in order to obtain the largest possible $K$ — and thus the lowest possible $u_s d_s$ product according to (4) — the current density as the cathode should be high and the cathode temperature as low as practicable.

### Some practical data compared with theory

To test the theory given in the foregoing we shall now make a simple calculation on the basis of data used in the design of an actucal picture tube. Under adverse conditions (bright environment) the average picture-brillance needed is about 100 nit (i.e. 29 ft L.) For a picture area of about 0.1 m² (e.g. a rectangular tube with a diagonal of 43 cm or 17″), the screen emitting diffuse light, this entails a luminous flux of $100 \times 0.1 \times \pi = 31$ lumens. The luminous efficiency of a fluorescent screen (without metal backing) can be put at approximately 10 lm/watt, so that the average power of the electron beam must be about 3 watt.

The voltage should be chosen as high as possible, having regard to spot sharpness (see equation 2). The practical limits are set here by safety requirements and considerations of size and cost price. In the tube to be described the accelerating voltage is 14 kV.To obtain a power of 3 watt we therefore need an average current of 0.2 mA. The permissible average load on the oxide cathode used is about 0.5 A/cm$^2$. If the cathode temperature is also known, we now have the data required for determining $K$. The temperature of the oxide cathode being about 1100 °K, the value of $K$, according to (7), is:

---

[2]) D. B. Langmuir, Proc. I. R. E. 25, 977-991, 1937.

[3]) J. Dosse, Z. Phys. 115, 530-556, 1940.

[4]) M. Ploke, Z. angew. Phys. 3, 441-449, 1951, and 4, 1-12, 1952.

$$K = 3.3 \times 10^7 \; V^{-1} \, \text{m}^{-2}.$$

Assuming further that the beam angle at the screen is restricted to $2 \times 10^{-3}$ rad in order to avoid excessive deflection-defocussing, we can calculate the theoretical diameter $d_s$ of the spot on the screen as 0.8 mm. In practice, however, diameters are found that are 1·5 times as large.

We can try to ascertain what causes this widening of the spot. Our electron-optical considerations lose their validity if the electron paths can no longer be considered as paraxial and if space charge phenomena occur. In the first case, spherical aberration can become serious in the triode section and in any prefocussing lens that may be provided. Spherical aberration in the final lens may reasonably be neglected for such narrow beams as these. From Ploke's [4]) calculations it appears that a 25% increase in beam diameter can occur in the triode section as a result of spherical aberration. The spot on the screen is therefore enlarged by the same amount.

The inherent space charge of the beam also gives rise to some widening, which is difficult to calculate exactly. An approximative method by Wendt [5]) gives a widening of 15% for the example under discussion.

After accounting for both these errors of image formations, the agreement between theory and experiment is quite satisfactory.

We shall now devote our attention in particular to the electron gun, first entering rather more closely into the question of prefocussing.

## Closer consideration of prefocussing [6])

As stated, the image quality of a picture tube is determined to a large extent by the width of the beam in the deflection coils: the less the width the less the deflection defocussing (see the article quoted in 1). The amount of deflection defocussing for a given beam diameter $d_D$ us determined by the radius of curvature of the screen and by the quality of the deflection coils. *Fig. 6* shows the focussed size of spot $d_s$ as a function of the distance $l$ from the middle of the screen, for tubes with a screen diagonal of 43 cm (17″) and two widths of beam, narrow and wide respectively. Apart from the gun, both tubes are identical. Curve $a$ refers to the narrow beam, curve $b$ to the wide. We see that the tube with the wide beam is better in the middle than the tube with the narrow beam. This agrees with the paraxial theory, according to which $d_s$ in the middle of the screen is inversely proportional to $u_s$ — the parameters of the cross-over and the anode potential $\Phi_s$ being constant. However, the narrow beam (curve $a$) gives a more sharply focussed picture at the edge of the screen. In addition to deflection defocussing, there is usually some "modulation defocussing" to be reckoned with. This may be accounted for as follows. If, after having focussed the electron beam at a specific current, we proceed to increase the current (in practice by varying the voltage on the control grid) two effects are produced. In the first place the cross-section of the cross-over (and thus of the "object") becomes larger in the triode lens as a result of spherical aberration and space charge phenomena, and therefore the spot on the screen also becomes larger. In the second placed the reduced power of the triode lens with a less negative grid causes the cross-over to shift towards the screen, so that the position of the object is changed and the beam is no longer focussed on the screen. Modulation defocussing is greater the narrower we make the beam. This can be seen in *fig. 7* where the size of the spot in the middle of the screen is plotted as a function of the beam current $I_s$ (drawn lines), the tube

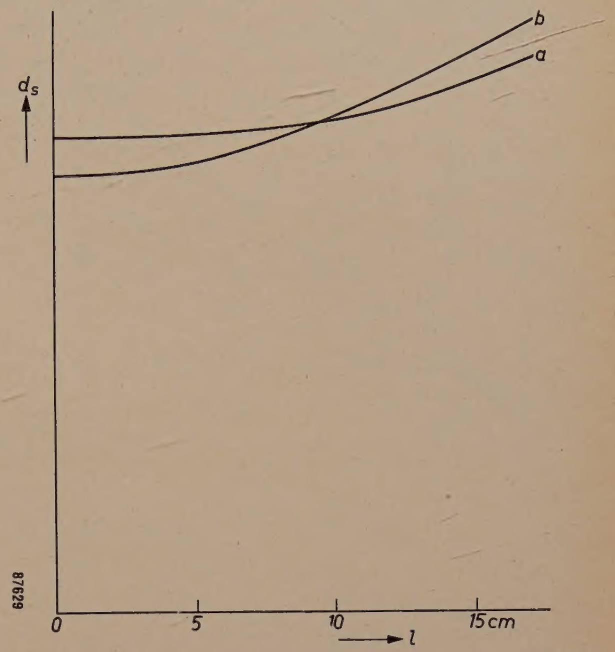

Fig. 6. The diameter $d_s$ of the focussed spot as a function of its distance $l$ from the middle of the screen; $a$ for a narrow beam, $b$ for a wide beam.

---

[5]) G. Wendt, Ann. Physik 2, 256-264, 1948.

[6]) An important contribution to the development about to be described was made by W. F. Niklas, now with Columbia Broadcasting System.

again being the 43 cm type and the focussing magnet being set for one specific beam current, in this case 100 μA. The broken lines indicate the size of spot when the beam is focussed for each value of the current, which is, of course, not the case in practice.

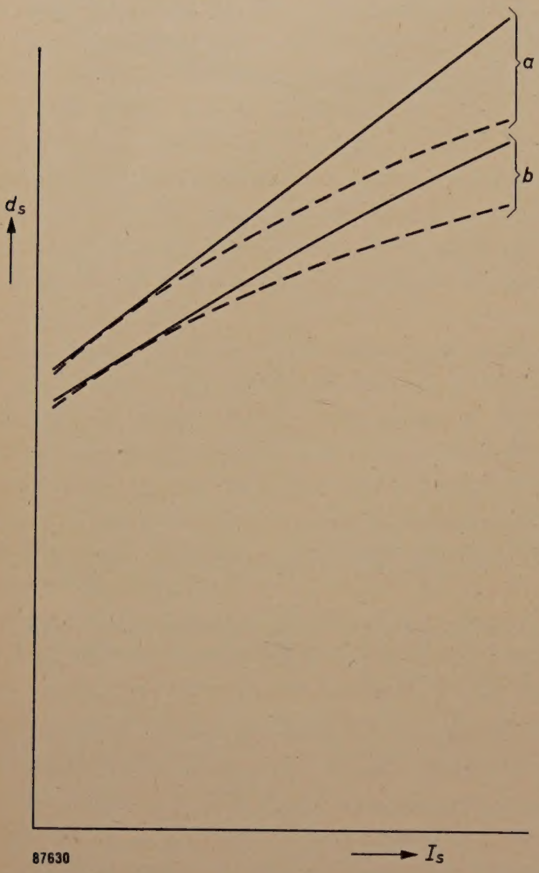

Fig. 7. The spot diameter $d_s$ at the middle of the screen as a function of the beam current $I_s$; *a* for a narrow beam, *b* for a wide beam.

Curves *a* and *b* refer to a narrow and wide beam respectively. The average slope of these curves is thus a measure of the modulation defocussing, and we see that the slope is somewhat flatter for the wide than for the narrow beam. The explanation of this phenomenon is too complicated to be included in this paper.

It will be shown below that the use of a pentode gun allows us in a given tube to vary within certain limits the compromise between the definition at the edge and that in the middle of the screen.

## The position of the prefocussing lens

We have shown that, according to the paraxial theory, it is immaterial where the prefocussing takes place. However, there are three reasons for positioning the prefocussing lens as close as possible to the triode section:

1) The closer the prefocussing lens to the triode section, the greater will the power of the lens have to be in order to obtain the same width of beam. It is known that spherical aberration in electron lenses generally decreases according as the focal length is reduced.
2) It is advisable to limit as much possible the area in which the electrons travel at a lower velocity and in which, therefore, the space charge causes greater divergence.
3) Owing to constructional restrictions in the diameters of the lens electrodes, it is advisable to keep the beam width in the prefocussing lens as small as possible in order to minimize aberrations of the image.

## The form of the prefocussing lens

Some possible forms of prefocussing lens are shown in fig. *8a, b and c*. The version generally adopted in television tubes until fairly recently is represented in fig. 8*a*. There are two parameters

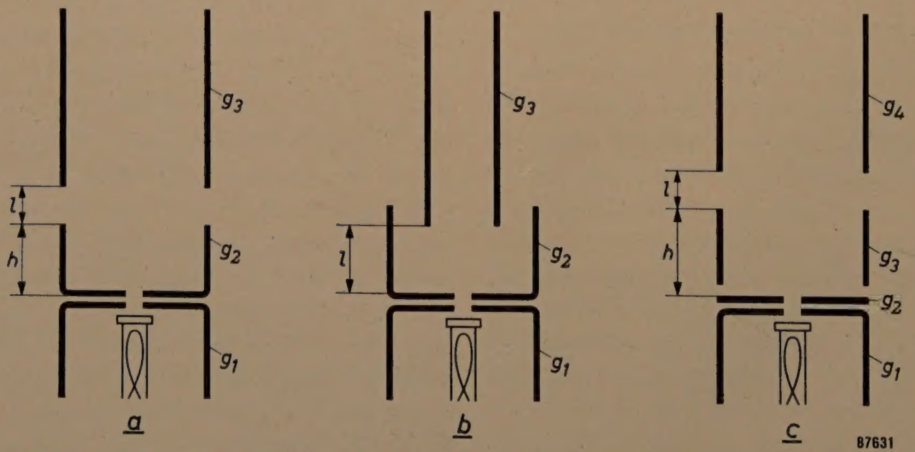

Fig. 8. Three possible versions of a gun with prefocussing lens. *a*) Tetrode gun, in which $g_2$ and $g_3$ have the same diameter, *b* the same, but $g_2$ and $g_3$ have different diameters, *c*) pentode gun.

that are mainly responsible for prefocussing the beam, viz. the distance $l$ between the first anode $g_2$ and the final anode $g_3$, and the height $h$ of the first anode.

The power of the lens is also affected by the diameter of the first anode; a smaller diameter gives a more powerful lens. In practice, however, the choice of diameter us restricted, outwardly by the size of the neck and inwardly by the risk of spherical aberration.

By changing the distances $h$ and $l$, the power of the lens and hence the focal length are changed. Both $h$ and $l$, when increased, cause greater prefocussing, but an increase in $h$ has more effect than the same increase in $l$. To keep the lens short, $l$ is made as small as possible without running the risk of field emission — the potential difference between the electrodes $g_2$ and $g_3$ can be as much as 20 kV — while the value of $h$ to give the requisite prefocussing is determined. A useful measure of the prefocussing, and one that can easily be verified experimentally, is the diameter of the spot on the screen, $d_V$, which is obtained without bringing the focussing lens $f$ into action (see fig. 3). With a given type of tube, the diameter $d_D$ of the focussed beam in the deflection coils is reasonably proportional to $d_V$. The diameter $d_D$ has an important bearing on the amount of deflection and modulation defocussing, as described. *Fig. 9a* shows $d_V$ as a function of $l$, for various values of $h$.

A second possible prefocussing lens is represented in fig. 8*b*; here the final anode is smaller in diameter than the first anode and is enclosed by the latter. The power of the lens is now determined by the distance $l$ and the ratio of the diameters of both anodes. Although this solution has been put into practical use, it has the drawback that the distance $l$ is difficult to adjust during assembly owing to the first anode being entirely enclosed by the final anode. Fig. 9*b* shows the spot diameter $d_V$ as a function of the distance $l$, for the case in which the ratio of the diameters is 1 : 2.

A third possibility is given in fig. 8*c*. This principle, which is now being applied in the design of almost all Philips picture tubes, entails the introduction of a fifth electrode. Suppose that in fig. 8*a* we cut through the first anode just above the base and then place the separate cylinder thus obtained a small distance away from $g_2$. If we now bring the annulus $g_2$ and the cylinder $g_3$ to the same potential as $g_2$ in fig. 8*a*, there will be practically no change in the action of the lens, when the distance between $g_2$ and $g_3$ is very small. However, if the potential on the cylinder is made to differ from that on $g_2$, the power of the lens will certainly change; the prefocussing lens will be more powerful when $V_{g3} < V_{g2}$ and weaker when $V_{g3} > V_{g2}$. If $V_{g2}$ remains unchanged, the modulation characteristic of the tube is not affected. We now have an electron gun with variable prefocussing, so that by regulating the voltage on $g_3$ we can achieve the best compromise between spot size and deflection defocussing.

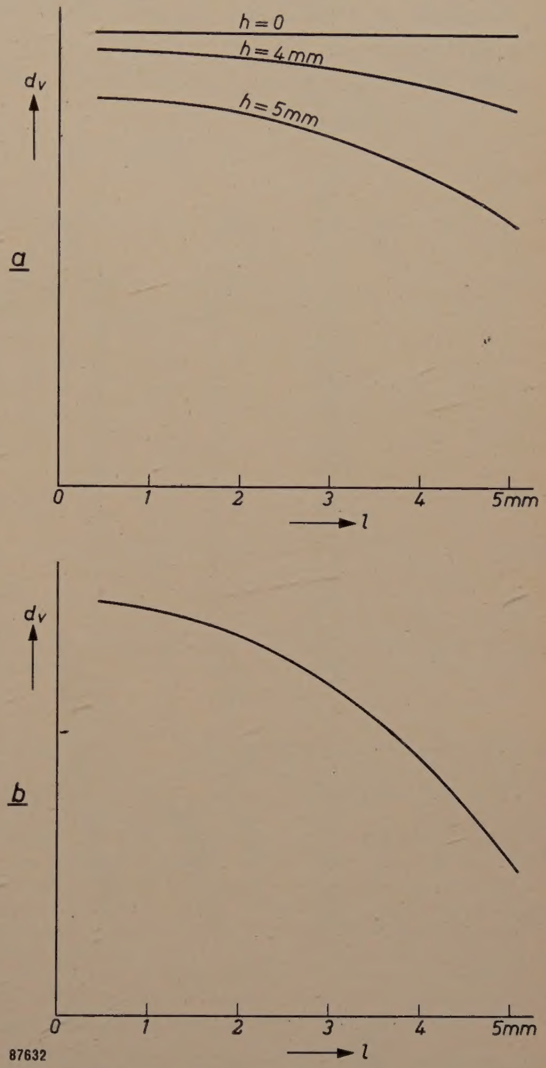

Fig. 9. *a*) The diameter $d_V$ of the unfocussed spot as a function of the distance $l$ between $g_2$ and $g_3$ for a gun as in fig. 8*a*. The parameter $h$ is the length of $g_2$. *b*) $d_V$ as a function of $l$ for a gun as in fig. 8*b*.

### Practical version of the pentode gun

During the design of the new gun incorporating the prefocussing lens as in fig. 8*c*, the voltage on $g_2$ was found to have a considerable influence on the power of the lens. This had to be avoided, since it would leave the designer less freedom in his choice of $V_{g2}$. The method adopted was to provide the cylinder $g_3$ with a base, as shown in *fig. 10a*, as a result of which the field of $g_2$ is prevented from penetrating so far into the space between $g_3$ and $g_4$. Fig. 10*a* illustrates the layout of the electrodes in the gun finally constructed. Electrode $g_3$ is slightly rounded and fitted with a plate to counteract field emission to the high-potential electrode $g_4$. All electrodes are mounted on ceramic rods, one of which can be seen in the figure [7]). Electrode $g_4$ is bent off-axis to provide, in conjunction with a permanent magnet, an ion trap [8]). The lower end of this electrode is terminated by an annular cap which determines the correct separation from the other electrodes. Springs are fixed to the top end for the purpose of centring the electrode in the glass envelope. A photograph of the gun is shown in fig. 10*b*. The ring visible above electrode $g_4$ contains a getter.

The voltage on $g_2$ can now be varied within fairly wide limits without seriously affecting the power of the prefocussing lens. The electrode $g_3$ must be so designed that the voltage on this electrode can be obtained without difficulty from the power pack. The voltages used in practice are therefore between — 50 and + 350 V. Since $g_3$ draws no current, its potential can readily be adjusted with a potentiometer. In this way, the width of the beam can be varied by a factor of 1·5, which is more than enough for the beam widths needed in practice.

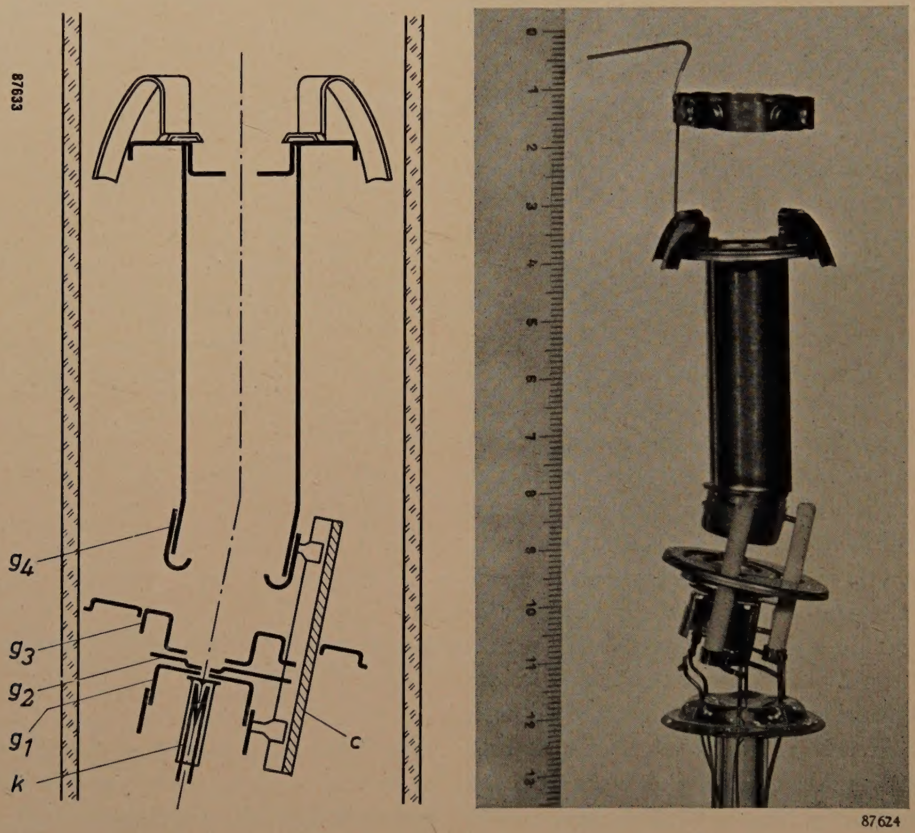

*a* *b*

Fig. 10. *a*) Structure of a pentode gun. The gun is mounted on three ceramic rods *c*. Electrode $g_4$ is centred with respect to the glass envelope by springs at the top. The bend in this electrode, in conjunction with a permanent magnet, serves as an ion trap.
*b*) Photograph of the finished gun.

Owing to the differences in the line systems and bandwidths used in European countries it is desirable to be able to vary the size of the spot on the television screen. For the English system of 405 lines the spot on the screen can be somewhat larger than for the Gerber system of 625 lines, and an even smaller spot is needed for the French system of 819 lines. In a television receiver intended for the English system, the prefocussing electrode $g_3$ should, as a rule, be given cathode potential ($V_{g3} = 0$ V) which results in a larger spot. The strong prefocussing further produces a narrow beam, the advantage of which is a spot of very uniform size all over the screen, even at the edges (very little deflection defocussing). This allows us to simplify the deflection coils to some extent, which slightly increases the deflection defocussing but does not impaire the quality of the picture. The designer may then devote rather more attention to obtaining a good rectangular form of raster, a requirement opposed to that of small deflection defocussing. This setting does, however, cause a slight increase in modulation defocussing. With the beam currents concerned, the spot is not noticeably enlarged thereby, but it is a reason for not decreasing $V_{g3}$ still further.

---

[7]) This construction is described by J. de Gier and A. P. van Rooy in Philips tech. Rev. **9**, 180-184, 1947/48.

[8]) See W. F. Niklas, Philips tech. Rev. **15**, 258-262, 1953/54.

For the 819 line system the procedure is just the opposite. Electrode $g_3$ is given a potential of about 300 V (e.g. by connecting $g_3$ with $g_2$). The spot in the middle of the screen is then as small as possible and there is also very little modulation defocussing. Owing to the beam being wider, however, the designer has to pay closer attention to coil design in order to avoid excessive deflection defocussing.

It is clear that the pentode gun allows the set designer to vary the properties of the gun to suit his design. The gun is little more complicated than its predecessors, which means that the additional facilities it offers need hardly affect the price of the set.

*Fig. 11* shows the size of the focussed spot $d_s$ (broken lines) and of the unfocussed spot $d_v$ (drawn lines, on a 10× larger scale) as a function of the prefocussing potential $V_{g3}$, at a beam current of 100 μA, for the three values of $V_{g2}$. As we have said, $d_v$ is a good measure of the beam width in the deflection coils. The figure confirms that with increasing $V_{g3}$ the beam becomes wider and the spot smaller. The curves given were plotted from data obtained from a type MW 43-64 tube; analogous curves apply to other types of tube, e.g. MW 36-44 and MW 53-20.

To conclude, some other interesting aspects of the pentode gun deserve mention, even though their value may be only theoretical. As explained in the foregoing, it would be desirable, having regard to modulation defocussing, to be able to focus the electron beam for each value of beam current.

It is obvious that, with a permanent focussing magnet as frequently used at the present time, such additional adjustment is not practicable. When using the pentode gun, however, the possibility exists of making the appropriate correction by means of an auxiliary voltage on $g_3$ derived from the modulation signal.

A similar means of reducing deflection defocussing would be to modulate $g_3$ with a voltage derived from the deflection currents — dynamic focussing. Naturally, this would only reduce the errors due to field curvature; it would not correct astigmatism. Both improvements require an extra circuit, which will probably be found too intricate for general use.

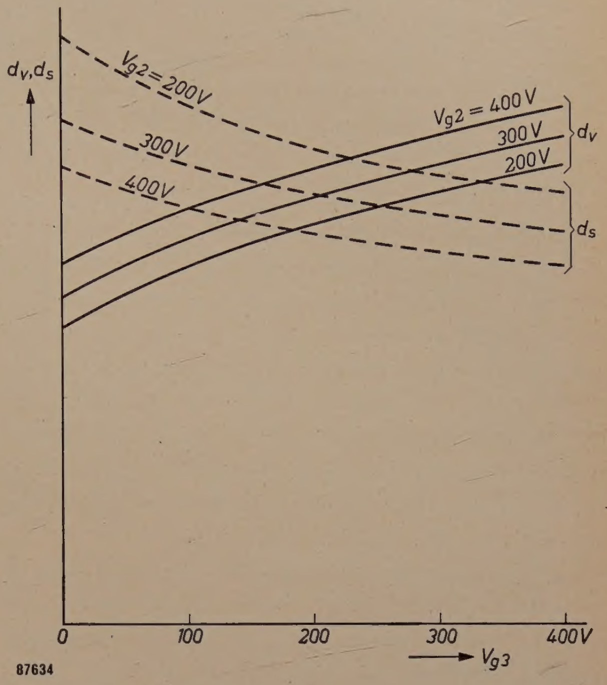

Fig. 11. The diameter $d_v$ of the unfocussed spot (full lines) and $d_s$ of the focussed spot (broken lines) as a function of $V_{g3}$, for various values of $V_{g2}$ ($d_s$ on a scale 10× larger than $d_v$).

**Summary.** When designing a television picture tube it is necessary to make the spot on the screen so small that the definition of the picture is determined by the television raster alone. This imposes certain demands upon the electron gun, which forms the beam. The beam is required to be as narrow as possible, because deflection defocussing increases with the diameter of the beam in the deflection coils. Consideration of the electron optics reveals the principal possibilities. Only the product of beam angle and spot size occurs in the equations and this product becomes smaller with increasing screen potential and current density at the cathode. If spherical aberration and space charge phenomena are taken into account, the values obtained in practice are in fairly good agreement with the theory.

Closer consideration is then given to the prefocussing lens. This should be positioned as near as practicable to the cathode. Examination of various possible forms of prefocussing lenses has led to the development of a pentode gun, which is now being used in almost all Philips picture tubes. Varying the voltage on the third electrode changes the width of the beam and the size of the spot on the screen, thus enabling the optimum size of spot to be chosen to suit the line system in use. It also allows a very narrow beam to be employed with a fairly coarse line system, which means that the deflection coils can be simplified without causing excessive deflection defocussing. Finally, the pentode gun makes it possible in principle to apply partial correction of deflection and modulation defocussing.

# AMPLITUDE MODULATION OF CENTIMETRE WAVES BY MEANS OF FERROXCUBE

by H. G. BELJERS.

621.376.2:621.396.029.64:621.318.134

---

*The Ferroxcube discussed in this article is mainly used as magnetic core material for frequencies up to about 100 Mc/s. At higher frequencies, phenomena occur which prevent its use as core material but which have led to a further, interesting application. This is one of those cases not infrequently occurring in technology where a particular discovery or a certain product is found to be applicable in a field different from that for which it was originally intended.*

---

Radio waves with a wavelength of less than about 30 cm have acquired considerable importance over the last ten years or so for experimental work in widely different scientific fields. Some examples are: microwave spectroscopy, gyromagnetic resonance phenomena and radio-astronomy. The most important industrial applications are radar and beamed communication links. For distances of 10 km or more absorption in the atmosphere precludes the use of wavelengths of less than 3 cm.

In radio communication, the transmission of information is effected by modulating a carrier wave and in principle we may use either frequency modulation (FM) or amplitude modulation (AM). Amplitude modulation may be effected by varying the voltage on one of the electrodes of a transmitting tube but it is generally accompanied by an interfering frequency modulation. Consequently it is preferable to bring about amplitude modulation in another manner e.g. by absorption. In this method the modulation is effected outside the transmitting tube; a varying fraction of the HF power is absorbed in the output circuit.

Study of the magnetic properties of ferrites has shown that in an H.F. magnetic field these materials are subject to losses dependent upon the frequency and the type of ferrite and also that these can be influenced by an external magnetic biassing field 1). This work, originally extending to frequencies of a few hundred Mc/s, has since been extended to much higher frequencies and it has been shown that the magnetic losses still occur up to about 10,000 Mc/s. From observations by W. J. van de Lindt in the Philips Laboratories at Eindhoven it has been found that, with a number of ferrites, weak external magnetic fields can produce large variations in these losses; hence by low frequency variation of the external field we should, in principle, be able to bring about an absorption modulation 2).

To achieve a modulation of this type a small ferroxcube rod may be fitted into a cylindrical cavity resonator as shown in *fig. 1a* at a point where the alternating magnetic field is strong. Fixed round the rod are coils by means of which a modulating magnetic field can be excited in the axial direction. The cavity resonator is coupled to a wave-guide through which the H.F. energy to be modulated flows. If the cavity resonator is tuned to the frequence of the wave in the guide (by adjusting the

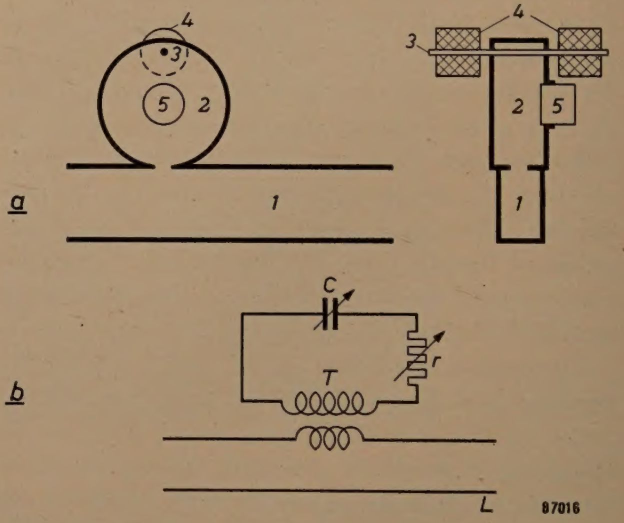

Fig. 1. Arrangement for "absorption modulation". *a*) the ferrite rod *3*, fixed in the cavity resonator *2* which can be tuned by the plunger *5*, can be magnetized by the coils *4*, thereby causing variations in the losses in the cavity resonator. Owing to the coupling with the wave-guide *1*, the power transmitted in the wave-guide varies.
*b*) Equivalent circuit of the arrangement. The cavity resonator, represented as a series resonant circuit coupled to a line *L*, is tuned by the variable capacitor *C*. The coupling between wave-guide and cavity is represented by the transformation ratio of the transformer *T*. The variable losses are represented by the variable resistor *r*. When *r* varies, the *Q* of the circuit changes, thereby altering the impedance in the line *L* and thus the amount of reflection that occurs.

---

1) H. G. Beljers and J. L. Snoek, gyromagnetic phenomena occurring with ferrites, Philips tech. Rev. **11**, 313-322, 1949/50.

2) H. G. Beljers, W. J. van de Lindt and J. J. Went, A new point of view on magnetic losses in anisotropic bars of ferrite at ultra high frequencies, J. appl. Physics, **22**, 1506, 1951.

plunger 5) the energy is partially reflected at this point: the higher the $Q$ of the cavity resonator, the greater the amount reflected. The equivalent circuit fig. 1*b*, illustrates the arrangement further. By varying the current through the coils, the $Q$ of the cavity resonator can be altered since the changing magnetic field causes variations in the losses of the ferroxcube. This, in turn, varies the amount of reflection and hence the amplitude of the wave passing through the wave-guide is modulated. Although the modulation cannot be attributed to direct absorption of the H.F. power to be transmitted but to a reflection controlled by absorption of a fraction of the power, we shall continue to refer to it here as absorption modulation.

Ferroxcube IVA and ferroxcube IVB have been used with success in this manner for a wavelength of 3.2 cms (9,300 Mc/s). In the following we shall show that the saturation magnetization of the ferroxcube determines the highest carrier frequency at which absorption modulation is possible. So far, no types of ferroxcube have been found possessing a sufficiently high saturation to permit modulation at carrier frequencies higher than about 12,000 Mc/s.

Using the experimental arrangement for 9,300 Mc/s mentioned above, a reasonable modulation was attained up to a modulation frequency of 1.3 Mc/s. At higher modulation frequencies it proves difficult to excite the desired low frequency field in the ferroxcube because the capacitance between the windings of the coils becomes considerable and leads to a weakening in the field.

Although, therefore, this modulation method cannot be considered for bandwidths larger than a few Mc/s it nevertheless affords interesting possibilities for using ferroxcube at very high frequencies [3]).

The phenomena that arise will be discussed in more detail below.

## Magnetic losses in ferrites

The magnetic losses of ferrites in an H.F. field may be regarded as being a result of gyromagnetic resonance.

Consider a body with a certain spontaneous, magnetic moment. Such bodies do exist, viz. the so-called Weiss domains in a ferromagnetic material (regions of dimensions of 0.1 μ to 10 μ) where all electron spins are roughly in the same direction. If the body is placed in a constant magnetic field $H$ making a certain angle with the magnetic moment, then, as explained in [1]) the vector of the magnetic moment precesses about the field direction with an angular frequency $\omega_p$ where

$$\omega_p = \gamma H . \quad . \; . \; . \; . \; . \; . \quad (1)$$

The constant $\gamma = 2.2 \times 10^5$ m/Asec is termed the gyromagnetic ratio. This relation holds so long as the precessing magnetic moment itself has no effect on the effective field $H$ (i.e. if no demagnetization occurs). This is the case with a spherical body. If we now apply a small HF magnetic field perpendicular to $H$, the angle of precession increases but for it to do so, energy has to be supplied from the HF field to the spin system: the magnetic moment is, as it were, bound with a certain coupling to the direction of the magnetic field $H$. If the alternating field has exactly the angular frequency $\omega_p$ of the precession, resonance occurs and the magnetic vector precesses at a greater angle with respect to the field direction, which corresponds to the least amount of energy. The precession energy absorbed when an alternating field is applied, is, however, partially transferred to the crystal lattice by interaction with it and this results in an increase in the temperature of the material: a part of the H.F. power is converted into heat and losses occur in the H.F field.

Closer investigation shows that in a ferromagnetic material resonance losses occur even without an external constant field. The magnetization in each Weiss domain has a preferential direction, namely that in which the lattice energy is minimum. The magnetization is bound to this state of equilibrium with a certain coupling, which causes it to describe a precessional movement with an angular velocity proportional to the strength of this coupling. Denoting this precession frequency $\omega_p^{(A)}$, we can introduce an equivalent field $H_A$ which for small deflections would give rise to the same coupling, so that we obtain

$$\omega_p^{(A)} = \gamma H_A . \quad . \; . \; . \; . \; . \; . \quad (2)$$

If an alternating external magnetic field having the same (or practically the same) angular frequency is now applied, the component of that field perpendicular to the equivalent field $H_A$ can cause resonance just as in the case where a constant external magnetic field $H$ is applied. In this case, too, energy is constantly being supplied from the H.F. field to the spin system, thereby giving rise to the development of heat.

The greater the forces due to the crystal structure (so-called anisotropic forces), the more difficult it is to direct the spins by an external magnetic field; the crystal forces are roughly inversely proportional to the susceptibility. With larger anisotropic forces we have a higher precession frequency; this implies that losses are noticeable only at higher frequencies. In ferrites, crystal anisotropy gives rise to losses which have their maximum value at frequencies between 2 and 200 Mc/s, according to [1]) and experiments confirm that the losses start to appear at higher frequencies at the susceptibility becomes smaller [4]).

---

[3]) An instance of this was described a short while ago in this review: J. Cayzac, Automatic frequency stabilization for a beam transmitter working on centimetric waves, Philips tech. Rev. **17**, 334-339, 1955/56.

Magnetic losses in ferrites are experimentally found up to about 10,000 Mc/s. This can be understood as follows. In each Weiss domain exists the saturation magnetization $M$. When no external magnetic field is present these magnetizations have a different direction from domain to domain, so that viewed as a whole, the material has no magnetic moment. Because the Weiss domains — each separately completely magnetized — vary a great deal in shape, demagnetizing effects will appear, differing in intensity from domain to domain, which can cause the coupling of the magnetic moment with the lattice (and consequently the gyromagnetic resonance frequency) to increase locally by considerable amounts (shape anisotropy).

Consider as an example a magnetized ellipsoid. The demagnetizing effect here is as small as possible provided the magnetic moment $M$ is in the direction of the major axis (state of least energy). The axis we term the $z$-axis. The magnetic moment is bound to this axis with a certain coupling and therefore here too a precession with a particular frequency $\omega_p'$ can appear. The magnitude of $\omega_p'$ depends, furthermore, upon the shape of the ellipsoid and it can be shown that the following relation applies:

$$\omega_p' = \gamma\sqrt{[H_A + (N_x - N_z)M]\,[H_A + (N_y - N_z)M]}. \quad (3)$$

where $H_A$ is the equivalent crystal anisotropic field (likewise assumed to be in the $z$ direction), $-N_xM$ is the demagnetizing field produced in the ellipsoid if the magnetization is in the $x$ direction, etc. In general we have,

$$N_x + N_y + N_z = 1.$$

For a sphere $N_x = N_y = N_z = \frac{1}{3}$; we see that $\omega_p' = \gamma H_A$; there is then no preferred direction and the precession frequency is the same as in a field $H_A$. With an ellipsoid $\omega_p'$ is generally higher. We find the highest frequency with an ellipsoid of revolution greatly elongated in the $z$ direction (needle). For this we have $N_x = N_y = \frac{1}{2}$ and $N_z = 0$, so that here

$$\omega_p' = \gamma(H_A + \tfrac{1}{2}M)\,. \quad . \quad . \quad . \quad . \quad (4)$$

Each Weiss domain in a ferrite shows a resonance curve and corresponding energy absorption round about a frequency of $\omega_p'$ which depends on the shape of the domain and can be approximately derived from equation (3) which holds for the idealized ellipsoidal shapes. By summing the losses of all domains at one frequency we obtain the losses of the material as a whole at that frequency. Since the needle-shaped domains are probably not very numerous, the losses will decrease with the frequency but will nevertheless exist up to the frequency given by (4). It can be seen from the fact that $M$ is of the order of $32 \times 10^4$ A/m (4,000 oersted) whilst the equivalent field $H_A$ amounts at most to $1.6 \times 10^4$ A/m (200 oersted) that this frequency is much higher than the resonance frequency corresponding to $H_A$. We find, moreover, from a closer analysis that even (4) still does not give the highest possible frequency, but that the precessional magnetisations of lamina-shaped Weiss domains occurring in particular superimposed strata, each with opposing magnetisation, influence each other [5]) and this causes the maximum frequency $\omega_{p\,max}$ at which losses can occur to increase to

$$\omega_{p\,max} = \gamma(H_A + M)\,. \quad . \quad . \quad . \quad . \quad (5)$$

This frequency is practically twice as high as that derived from (4) and amounts to 4,000—12,000 Mc/s for the various kinds of ferroxcube.

Consider now the influence of an external constant magnetic field $H$. We have already seen that with a sphere a resonance frequency $\gamma H$ occurs. What happens, however, with a thin rod such as is used in the arrangement described for absorption modulation? If we apply here a constant field $H$ parallel to the axis of the rod, even a small value of this field, e.g. 4,000 A/m (50 oersted) is sufficient to completely saturate the ferrite so that everywhere the magnetization $M$ is directed along the axis. If we disregard the crystal anisotropy field $H_A$ that varies locally in magnitude and direction, the whole rod behaves as one large needle-shaped Weiss domain with, according to (4), a resonance in the neighbourhood of the frequency

$$\omega_p^{(H)} = \gamma \cdot \tfrac{1}{2}M\,. \quad . \quad . \quad . \quad . \quad . \quad . \quad (6)$$

(The crystal anisotropy field $H_A$, and in general the external magnetic field $H$ too, are both small with respect to $\frac{1}{2}M$). The energy absorption of all parts of the rod is now concentrated in this frequency range so that the losses are much higher than in the case where there is no external magnetic field.

---

[4]) See J. L. Snoek, Physica **14**, 207-217, 1948.

[5]) D. Polder and J. Smit, Resonance phenomena in ferrites, Rev. mod, Phys. **25**, 89-90, 1953.

### Testing the theory; possible methods of modulation

The magnetic characteristics of ferrites are usually determined by measuring the complex relative permeability:

$$\mu_r = \frac{B}{\mu_0 H} = \mu' - j\mu'',$$

where the quantity $\mu''$ is a measure of the losses.

Two curves $p$ and $q$ are plotted in *fig. 2* which show measurements of $\mu''$ for Ferroxcube IV in the frequency range from 0.2 to 24,000 Mc/s. The external biassing magnetic field is zero for curve $p$; losses start here at approximately 0.5 Mc/s and have become relatively small again at 300 Mc/s but nevertheless, still exist up to frequencies of about 9,300 Mc/s. With curve $q$, the biassing field is 4000 A/m so that the ferrite rod is saturated. These measurements confirm the theory at least qualitatively. At saturation, the resonance frequency ($\omega_p^{(H)}$) for this ferrite amounts to roughly 5,000 Mc/s. In a demagnetized state, the losses are very small at frequencies higher than about 10,000 Mc/s.

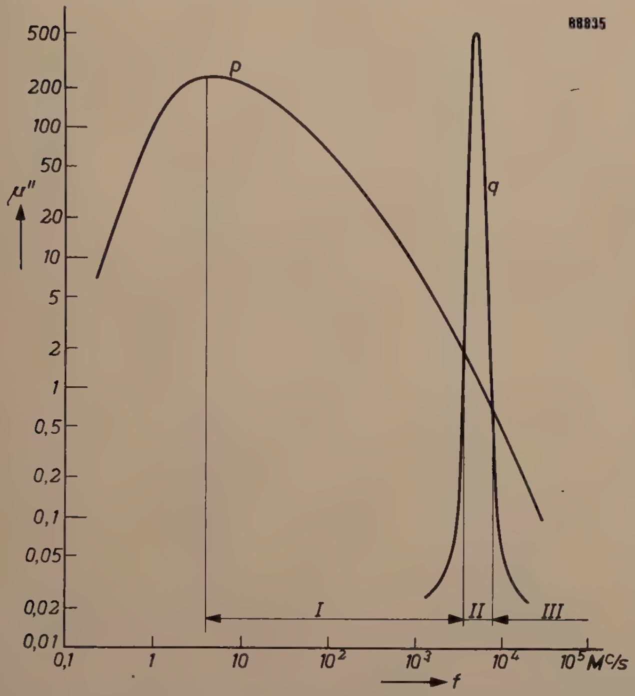

Fig. 2. The losses of an H.F. field in ferroxcube IVA expressed by the imaginary part $\mu''$ of the relative permeability as a function of the frequency: $p$ without a magnetic biassing field, $q$ with a saturating magnetic field.

On the basis of these loss curves, it is easy to understand how we can achieve absorption modulation by varying an external magnetic field. In each period of the modulating magnetic field, the loss curve alternates between the form $p$ and the form $q$ so that at a fixed carrier frequency the power absorbed varies periodically.

To consider this further, the frequency scale is divided into the regions *I*, *II* and *III* using the abscissae of the intersections of $p$ and $q$ as boundaries. Frequency range *I* includes the frequencies from about 100 Mc/s (the modulation method under consideration here is of no interest for lower carrier frequencies) to approximately 3,000 Mc/s. In practice, absorption modulation with ferrites is unlikely to be used in this frequency region since conditions are such that the resonance frequency (peak of loss curve) even at partial saturation by the external magnetic field becomes equal to the carrier frequency. With an increasing magnetic field the losses would first increase and then decrease, thereby giving rise to an undesirable modulation characteristic.

Absorption modulation is also not particularly suitable for region *II* since the losses do not drop to a low value for any value of the magnetic field when the latter remains small with respect to $M$. Absorption modulation is best suited to region *III*, viz. the highest frequencies, since with an increasing magnetic field the losses decrease steadily and drop to a low value with a saturating field.

In this connection, we must still bear in mind that $M$ (and consequently $\omega_p^{(H)}$) depends upon the temperature. If we wish the arrangement to maintain approximately the same modulation characteristic (in range *III*) in a broad temperature range, we must therefore remain sufficiently far away from the resonance peak. Because many kinds of ferroxcube exist having a different saturation

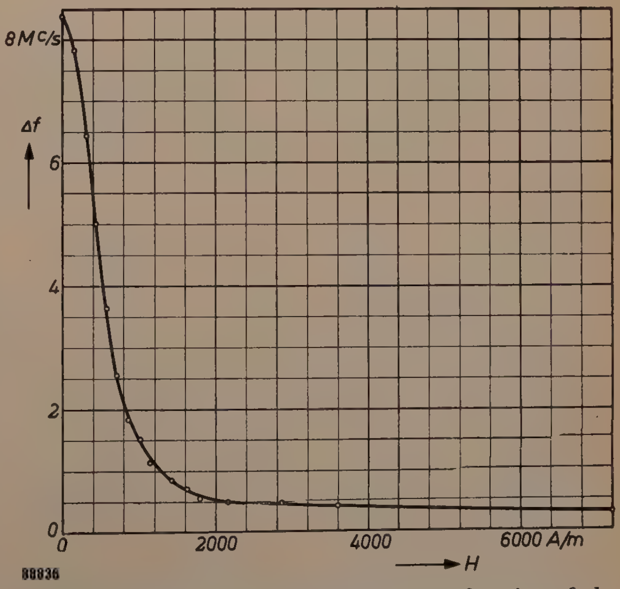

Fig. 3. The losses in an Mn-Mg ferrite as a function of the biassing magnetic field $H$ at 9,300 Mc/s. The half-value width $\Delta f$ of the resonance curve of the cavity resonator in which the ferrite is placed is plotted as the ordinate. This $\Delta f$ is proportional to the losses and hence to $\mu''$.

magnetization it is, however, possible to find the right ferroxcube for this modulation method for each carrier frequency between 2,000—12,000 Mc/s. In *fig. 3* the losses for a rod of Mn-Mg ferrite at 9,300 Mc/s are plotted as a function of $H$; this is therefore the modulation characteristic for that carrier frequency.

A further peculiarity may be noted here. It is a well-known fact that in the case of magnetic resonance the susceptibility is negative at frequencies above the resonance frequency (the magnetisation is then in anti-phase to the external field). When the resonances of all Weiss domains are superimposed on each other, the permeability $\mu'$ of the whole ferrite rod at certain frequencies therefore become smaller than unity. This is, in fact, the case close to the upper limit of the loss range, as can be seen a *fig. 4* where the real part $\mu'$ of the permeability for ferroxcube IVA is plotted as a function of the frequency over a wide frequency range. We observe that $\mu'$ decreases rapidly whenever losses occur (cf. curve $p$ in fig. 2), and before $\mu'$ approaches unity at very high frequency there is a range where $\mu' < 1$. (In order to delineate the curves clearly in each range, the scale of the ordinate is linear between 0 and 1 and logarithmic for values $> 1$).

Finally, we may give a quantitative experimental confirmation of formula (5) which shows the relation between the maximum frequency at which losses occur in a demagnetized state and the magnetization $M$ of the Weiss domains (saturation magnetization). Working with large frequency variations in the centimetre wave region is inconvenient; hence, instead of varying $\omega$, we may vary the saturation magnetization $M$, keeping the frequency constant. As already mentioned in the foregoing, this saturation magnetization depends on the temperature, as found from other measurements: the magnetization decreases as the temperature rises. The losses at 9,300 Mc/s for ferroxcube IVB and IVC are plotted in *fig. 5* as a function of the temperature. It can be seen that the losses in ferroxcube IVB become small at 120 °C and that this occurs at 160 °C for ferroxcube IVC. We also know that $M$ is approximately equal to $2.6 \times 10^5$ A/m (3,300 oersted) in both these cases. Thus we find experimentally that the maximum resonant frequency $\omega_{\max}$ is

$$\omega_{\max} \approx \gamma M,$$

in agreement with (5).

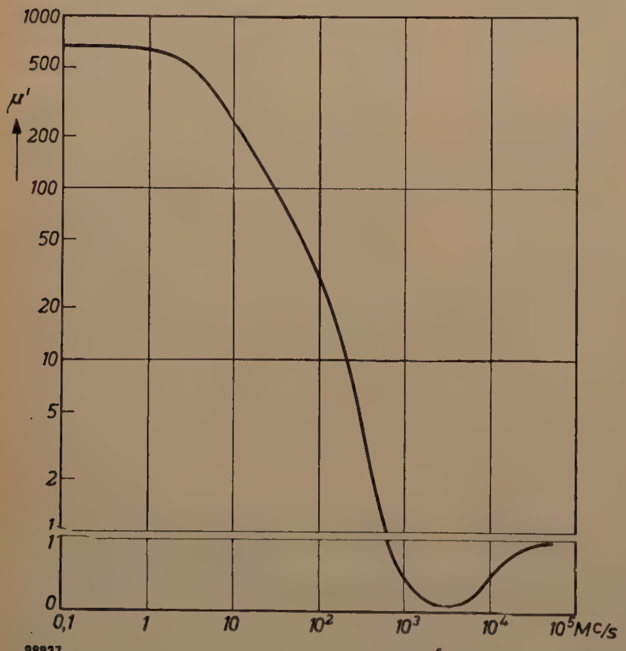

Fig. 4. The real part $\mu'$ of the relative permeability of ferroxcube IVA as a function of the frequency. Values below unity are plotted on a linear scale; above unity the ordinate is logarithmic.

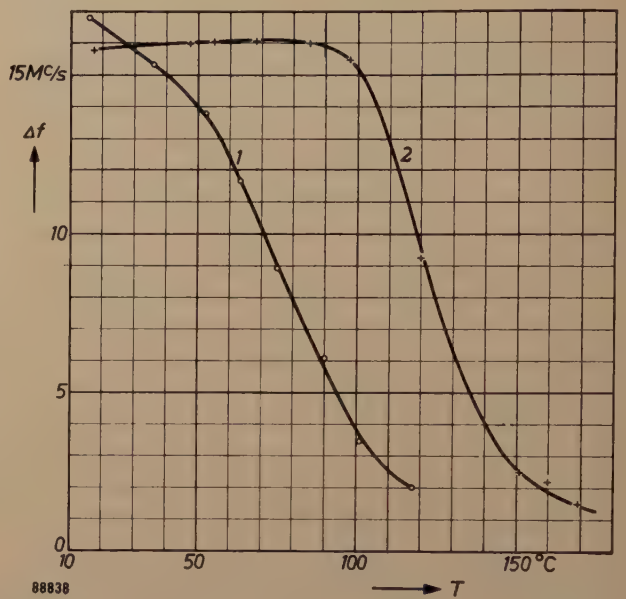

Fig. 5. The magnetic losses of ferroxcube IVB and IVC as functions of the temperature. The losses are expressed in terms of $\Delta f$ (see fig. 3).

**Summary.** A centimetre wave transmitter can be modulated by controlled absorption of the power transmitted. An absorption of this type can be brought about by gyromagnetic losses in ferrites. An H.F. magnetic field exhibits losses in demagnetized ferrites over a large frequency range, e.g. from 10—10,000 Mc/s. If, however, the ferrite is magnetized by a weak external biassing field the spin directions are aligned and the losses are concentrated in a small frequency region in the neighbourhood of a certain high frequency; outside this region the losses are small. If the external biassing field at a given carrier frequency is allowed to vary in intensity, variations in losses arise. These variations may be used for absorption modulation, allowing modulation up to frequencies of 1.3 Mc/s. The carrier frequency for this modulation can in principle be chosen between 2,000—12,000 Mc/s provided a type of ferroxcube is used which has a suitable saturation magnetization value. The nature of the losses is discussed; they arise through resonance phenomena under the influence of crystal anisotropy fields and internal magnetic fields that can assume different values by demagnetization. The experimentally found maximum frequency at which losses ocuur can also be explained theoretically.

# THE MEASUREMENT OF RADIOACTIVE IODINE IN THE THYROID GLAND

621.387.4:546.15.02.131:616.44-07

In the diagnosis of disorders of the thyroid gland use is often made of the radioactive iodine isotope $I^{131}$. The assimilation of iodine from the food is a measure of the activity of the thyroid gland and, in principle, can be easily investigated by administering a dose containing the radioactive isotope and determining the radioactivity of the thyroid on a number of consecutive days with, say, a Geiger counter tube.

In practice, determination of the radioactivity of the thyroid gland is a matter of some difficulty, at least if the accuracy is to be within a few percent, since the position of the source of radiation with respect to the radiation detector, i.e. the position of the neck of the patient with respect to the counter, must be exactly the same for each measurement. The problem has been solved by using a ring of counter tubes connected in parallel, fitting like a collar round the patient's neck. Radiation, emitted in all directions by the thyroid, is then integrated (at least in one plane), and should the source be off-centre, a loss in one counter tube will be roughly compensated by the increased radiation received by the diametrically opposite tube.

The instrument shown [1]) was made feasible by the use of a Geiger counter tube (type no. 18503) whose active volume comprises practically the whole length of the tube (5 cm including the anode connection). Ten such tubes have been accommodated without difficulty in the collar [2]). Moreover, the above-mentioned type of Geiger tube has the advantage of a low working voltage (less than 400 V) and a very flat plateau, so that it is not necessary to stabilize the voltage supply [3]).

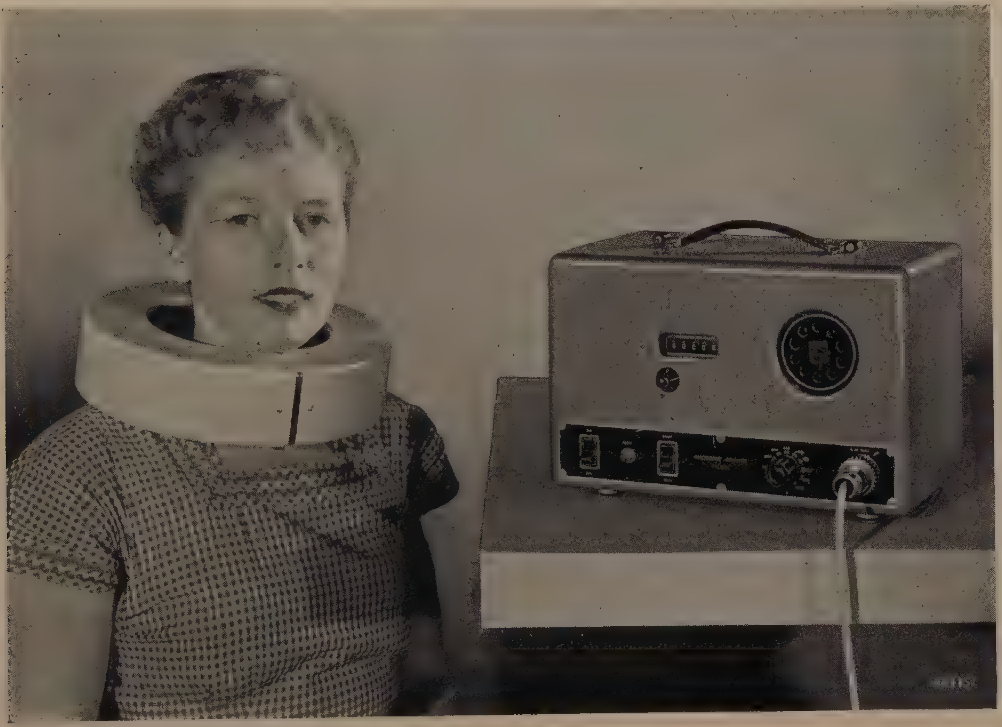

The collar is calibrated by means of a phantom. If a bottle containing 5 microcuries of $I^{131}$ — the order of magnitude of the $I^{131}$ taken up by the thyroid during actual investigations — be placed in the centre of the collar, about 700 pulses/minute are recorded. The background caused by cosmic radiation is about 100 pulses/min. With a phantom of the patient's neck, constructed from meat, with a bone as the spinal column and a small rubber bag filled with a solution of radioactive iodine as the thyroid, the count obtained is about 10% higher than that from the iodine solution alone. One cause of this higher reading is the secondary radiation generated particularly in the spinal column, which is better absorbed by the counter tubes. Such phenomena also result in a lower sensitivity to displacement of the source of radiation when the phantom is present; without a phantom 20% more pulses are obtained when the source of radiation is 4 cm off-centre, whereas with a phantom only 10% more pulses are recorded for a similar displacement.

---

[1]) A. M. J. Jaspers and H. R. Marcuse, Local measurement of $I^{131}$ uptake in the thyroid gland, Rec. Trav. chim. Pays-Bas **74**, 355-361, 1955 (No. 5). The apparatus has been in use for some time at the Municipal Hospital in The Hague.

[2]) Toroidal tubes, enclosing the whole neck, have been constructed for the same purpose; however, they are difficult to manufacture and for this reason have not been marketed; see W. Horst, Fortschr. Röntgenstr. 77, 567, 1952.

[3]) See: N. Warmoltz, Geiger-Müller counters, Philips techn. Rev. **13**, 282-292, 1951/52.

The discrepancy of 10% is still inadmissible, but variations in the positioning of the collar round the neck can be kept very much less than 4 cm during the series of repeated measurements. This is done quite simply by means of fitting-rings which slot into the collar and fit round the neck of the patient; see photograph above. The error due to variation in the positioning of the collar is reduced in this way to about 2%. In order to reduce the statistical measuring error to roughly the same level, the pulses produced by 5 μC must be counted over 15 minutes [4]). Usually the patient is given 20 μC which results in a counting time of 3-5 minutes.

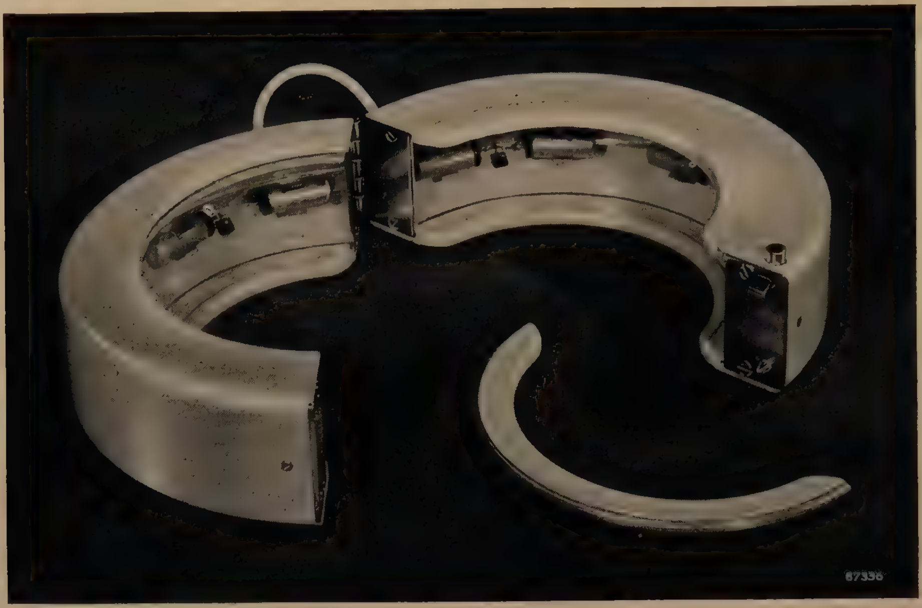

Further details as to the measurement and the diagnostic interpretation will not be gone into here, but it should be added that for accurate assessment of the amount of iodine in the thyroid, a correction must be applied to the results of the measurement for the amount of iodine in the blood flowing through the neck. This correction is found by recording the radioactivity with the collar around the thigh of the patient in conjunction with each measurement on the thyroid; from measurements on patients whose thyroids have been removed, the radioactivity measured at the thigh — where the count rate is 2-3 times the background — was found be to about $^2/_3$ that of the bloodstream through the neck.

A. M. J. JASPERS.

---

[4]) See for example, Philips tech. Rev. **17**, 206, 1955/1956 (No. 7-8).

# MECHANICAL PHENOMENA IN GRAMOPHONE PICK-UPS AT HIGH AUDIO FREQUENCIES

by J. B. S. M. KERSTENS.

534.851:681.842.081.3

*An article on a new gramophone pick-up will shortly appear in this review. As an introduction to this article we give here a study of the mechanics of the system pick-up - record, particularly at high audio frequencies. Extensive calculations on this question can be found in the literature; often, however, the physical aspect on the phenomena is liable to get lost and only after considerable simplification are useful results obtained. In this article the higher harmonics of the stylus motion are neglected at the outset, so that the mathematics does not cloud the general physical picture.*

Two phenomena are important in determining the frequency response of a pick-up in the higher audio range (about 5000 to 20 000 c/s). The first is the stylus-groove resonance, i.e. the resonance of the effective mass, thought of as concentrated in the stylus tip, and the stiffness of the walls of the groove in which the stylus rests. The second phenomenon is the loss of high notes owing to the elastic deformation brought about by the stylus tip in the walls of the groove, a loss that is greater the smaller are the radii of curvature of the groove walls, i.e. the higher the modulation frequency, the greater the amplitude and the nearer the pick-up is to the centre of the disc.

The theory of the elastic deformation of two curved bodies in mutual contact under the influence of a given force as given by Hertz[1]) can be applied to both phenomena. As early as 1941 Kornei[2]) developed a theory based on Hertz' work to explain the "playback loss" at higher frequencies.

On the basis outlined by Kornei, F. G. Miller[3]) developed a broadly conceived theory on the relations between groove and stylus. Apart from the deformation of the groove walls, he includes the distortion in the motion of the stylus when tracing a groove with perfectly rigid walls, in which he employs the calculations of Lewis and Hunt[4]). This tracing distortion arises from the finite dimensions of the stylus tip, so that the curve traced by the stylus is not entirely identical with that cut into the record. In this further analysis Miller splits up the complex motion of a stylus riding a sinusoidal groove into a fundamental component and higher harmonics; as regards the fundamental component he arrives at relatively simple formulae, from which are derived the phenomenon of stylus-groove resonance as well as the loss of high notes.

In order to gain a clearer picture of the physical phenomena, the higher harmonics will be disregarded here. We can thus confine ourselves to a greatly simplified derivation, keeping in mind, however, that this theory will not be entirely valid in extreme cases such as may occur sometimes in practice. This simplification also means that wherever we speak of deformations, these are considered to be of a purely elastic nature, according to Hooke's law. The highly complex phenomena occurring with plastic deformation do not lend themselves to a simple description[5]).

In the following considerations of the pick-up as a mechanical system only the trajectory of the stylus tip will be studied; resonances of the mechanical transmission system and of the electrical circuit will be disregarded.

## Deformation of the groove walls

Before dealing with the deformation of the groove walls by the reproducing stylus, let us first consider the geometry of the groove and the forces exerted by the stylus on the groove walls. Let us assume that a sinusoidal signal

$$y = \hat{y} \sin \omega t$$

has been recorded, the $y$-axis being chosen in the plane of the record, normal to the unmodulated groove. During playback the angular frequency is determined by the "wavelength" $\lambda$ registered in the record, and by the linear velocity $V_g$ of the groove, according to:

---

[1]) Heinrich Hertz, Gesammelte Werke, III. Die Prinzipien der Mechanik. J. A. Barth, Leipzig 1894; S. Timoshenko, Theory of elasticity, McGraw-Hill, New York 1934.

[2]) O. Kornei, On the playback loss in the reproduction of phonograph records, J. Soc. Mot. Pict. Engrs. **37**, 569-590, 1941.

[3]) F. G. Miller, Stylus-groove relations in phonograph records, dissertation, Harvard 1950.

[4]) W. D. Lewis and F. V. Hunt, J. Acoust. Soc. Amer. **12**, 348-356, 1940/41. See also: J. A. Pierce and F. V. Hunt, J. Acoust. Soc. Amer. **10**, 14-28, 1938/39.

[5]) F. V. Hunt, On stylus wear and surface noise in phonograph playback systems, J. Audio Eng. Soc. **3**, 2-18, Jan. 1955.

$$\omega = 2\pi \frac{V_g}{\lambda} . \quad . \quad . \quad . \quad . \quad . \quad . \qquad (1)$$

*Fig. 1* shows part of such a sinusoidal groove; the stylus tip, represented by a sphere, is situated here just at the crest of the wave. At this spot both lateral amplitude and acceleration are greatest, so that both stiffness force and inertia force will also be maximum. These forces can be represented respectively by

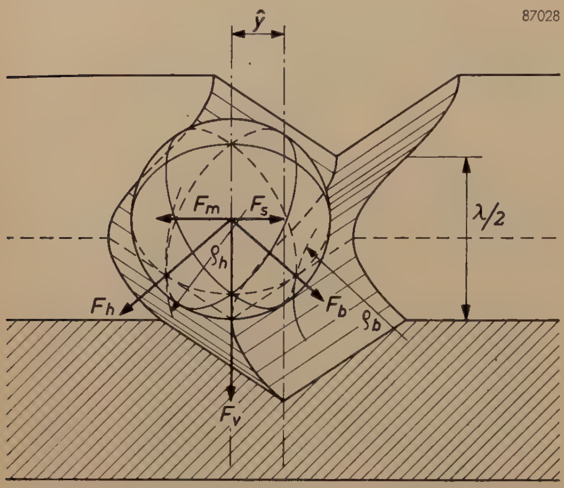

Fig. 1. The stylus tip, represented as a sphere, rests in the groove of a record, near the crest of the recorded sine wave. The walls of the groove are thought of as perfectly rigid.

$$\hat{F}_s = s\hat{y}_a \quad \text{and} \quad \hat{F}_m = m\omega^2\hat{y}_a, \quad . \quad . \quad . \qquad (2)$$

*s* being the stiffness and *m* the effective mass of the stylus system considered as acting through the centre of the stylus tip; $\hat{y}_a$ is the amplitude of the actual stylus trajectory, which will generally differ from *y*, as will be shown later (suffix a for "actual", because the curve representing $\hat{y}_a$ as a function of the frequency will be called the actual pick-up characteristic; see below). $F_s$—$F_m$ is the nett *lateral* force $F_l$ on the stylus tip.

Apart from this lateral force, a vertical force $F_v$ acts on the stylus tip. If we disregard the "pinch" effect [6]) the latter force can be considered as constant.

In the foregoing no mention has been made of the damping of the pick-up. In general, $F_l$ may be written as [7]):

$$F_l = \left(s + r\frac{d}{dt} + m\frac{d^2}{dt^2}\right) y_a , \quad . \quad . \qquad (3)$$

where *r* represents the damping of the pick-up. In *fig. 2* the two forces $F_l$ and $F_v$ are represented again, with their components at right angles to the groove walls.

The groove angle $2\beta$, being very nearly 90° in practice, is assumed, for the sake of simplicity, to be exactly 90°. For the forces normal to the groove walls we then obtain [8])

$$\left.\begin{aligned} F_h &= \tfrac{1}{2}\sqrt{2}\,(F_v + F_l) \\ F_b &= \tfrac{1}{2}\sqrt{2}\,(F_v - F_l) \end{aligned}\right\} , \quad . \quad . \quad . \quad . \qquad (4)$$

where the suffix h refers to the concave side of the groove and b to the convex side. These forces cause elastic deformations of the groove walls. The depth of the deformations is determined not only by these forces, but also by the nature of the materials and by the curvatures of the surfaces concerned. Evidently, a stylus tip with a small radius of curvature will penetrate deeper into the groove wall than one with a larger radius. It is likewise fairly obvious that a stylus tip of given radius will penetrate deeper into the convex than into the concave wall of the groove, since the contact area of the stylus with the latter is greater.

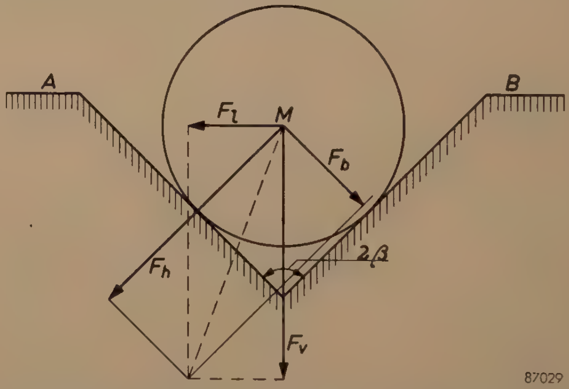

Fig. 2. Cross-section through the centre *M* of the stylus tip, for the situation shown in fig. 1. The groove-wall is concave at *A*, convex at *B*.

All this can be expressed in a formula given by Hertz for the elastic deformation of curved bodies in contact under a given force. For this special case the formula takes the form:

$$a = \left\{ \left(\tfrac{3}{4}\right)^2 F^2 \left(\frac{1-\sigma^2}{E}\right)^2 \frac{1}{R} \left(1 \pm \frac{R}{2\varrho}\right) \right\}^{\frac{1}{3}} . \quad . \qquad (5)$$

---

[6]) See e.g. Philips tech. Rev. **13**, 139, 1951/52.

[7]) If the method of complex numbers is used, $F_l$ may also be expressed as the product of the mechanical impedance at the stylus tip and the velocity $v = j\omega y_a$:

$$F_l = \left(\frac{s}{j\omega} + r + j\omega m\right) v . \quad . \quad . \quad . \quad . \quad . \qquad (3a)$$

[8]) In fig. 2 the direction of $F_l$ is to the left. This direction depends not only on the relative magnitude of $F_s$ and $F_m$ (the latter a function of frequency) but also on the damping, which introduces a phase angle between $F_l$ and $F_m$. The effects of these quantities on the direction of $F_l$ may be quantitatively examined by considering the mechanical impedance and the velocity as functions of the frequency; cf. eq. (3a) in footnote [7]).

The symbol $\alpha$ represents the depth of penetration, $F$ the force exerted by the stylus normal to the groove wall, $E$ and $\sigma$ respectively the Young's modulus and the Poisson's ratio of the record material (for both shellac and plastic records, $\sigma \approx 0.35$), $R$ the radius of the spherical tip of the stylus, and $\varrho$ the radius of curvature of the groove wall in a plane subtending an angle $\beta$ with the horizontal plane. In (5) the plus-sign applies to a convex groove wall, the minus-sign to a concave one.

In Hertz's original formula a term appears with Young's modulus of the stylus material (at present generally sapphire or diamond) in the denominator. This modulus, however, is so much greater than that of the record material that this term can be neglected; in comparison with the record, the stylus can be regarded as perfectly rigid. The relevant values of $E$ are roughly as follows [9]:

| Material | $E$ (newtons/m$^2$) |
|---|---|
| Plastic | $3 \times 10^9$ |
| Shellac | $6 \times 10^9$ |
| Sapphire | $500 \times 10^9$ |
| Diamond | $900 \times 10^9$ |

(The plastic referred to here is a copolymer of vinyl chloride and vinyl acetate [10]), commonly used for long-playing records.)

Substituting the values of $F$ given by (4) in (5) and grouping the constants together, we obtain for the penetration depths $\alpha_b$ and $\alpha_h$ in the convex and the concave side respectively:

$$\alpha_{b,h} = \left\{ \left(\tfrac{3}{4}\right)^2 \left(\frac{F_v}{\sqrt{2}}\right)^2 \left(\frac{1-\sigma^2}{E}\right)^2 \frac{1}{R} \right\}^{\frac{1}{3}} \left\{ 1 \mp \frac{F_l}{F_v} \right\}^{\frac{2}{3}} \left\{ 1 \pm \frac{R}{2\varrho} \right\}^{\frac{1}{3}} =$$

$$= \alpha_0 \left\{ 1 \mp \frac{F_l}{F_v} \right\}^{\frac{2}{3}} \left\{ 1 \pm \frac{R}{2\varrho} \right\}^{\frac{1}{3}}, \quad . \; . \; . \; . \quad (6)$$

where $\alpha_0$ represents the penetration depth in an unmodulated groove, since in this case $F_l = 0$ and $\varrho = \infty$.

It follows from (6) that the penetration depths can be reduced by increasing $E$ (in this respect shellac is to be preferred to plastic), by increasing $R$, or by reducing $F_v$. Later in this article we shall consider the effect of $F_l$ and $\varrho$.

*Fig. 3* shows a cross section of a stylus in an unmodulated groove indicating a typical static deformation. The value of $\alpha$ was derived from the values of $F_v$, $E$, $\lambda$ and $R$. *Fig. 4* is a perspective sketch of a stylus resting (stationery) in a *modulated* groove.

## Analysis of the stylus motion

The trajectory of the stylus can be studied with the aid of the following imaginary experiment. The pick-up rests in a stationary groove, e.g. at the crest of a sine wave, as shown in fig. 1. Because the penetration in the convex groove wall is deeper than in the concave one, the tracing sphere rests such that the horizontal distance of its centre from the zero line (centre of unmodulated groove) is not $\hat{y}$, as would be the case with a perfectly rigid wall (*fig. 5a*) but smaller, say $\hat{y}_s$ (s for the static situation considered) as in fig. 5*b*. If the stylus is exactly at the point where the groove passes through zero, the penetrations on either side will be equal, as the groove can be considered straight at this point. In this case, therefore, the horizontal projection of the centre coincides with the point of zero amplitude (*N* in fig. 5*b*).

Progressing accordingly for intermediate points, we arrive at a curve such as $y_s$ in fig. 5*b*. A loss in

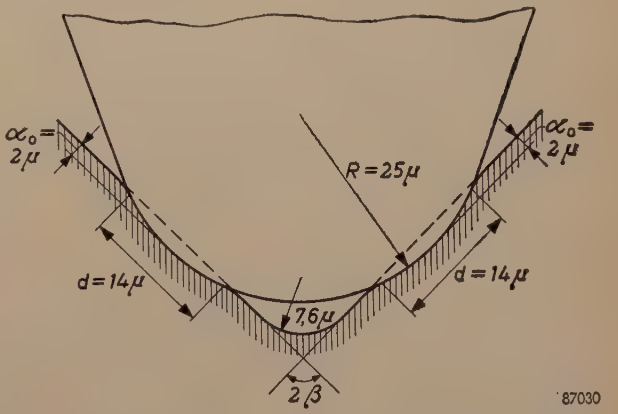

Fig. 3. Elastic penetration by the stylus in the walls of an unmodulated groove, drawn to scale for a co-polymer plastic record with $E = 3.3 \times 10^9$ N/m$^2$ and $\sigma = 0.35$. Groove angle $2\beta = 90°$. Apex angle of stylus 45°. Vertical force $F_v = 0.1$ N ($\approx 10$ g). Depth $\alpha_0$ of the penetration is 2 $\mu$, diameter $d$ of contact area is 14 $\mu$.

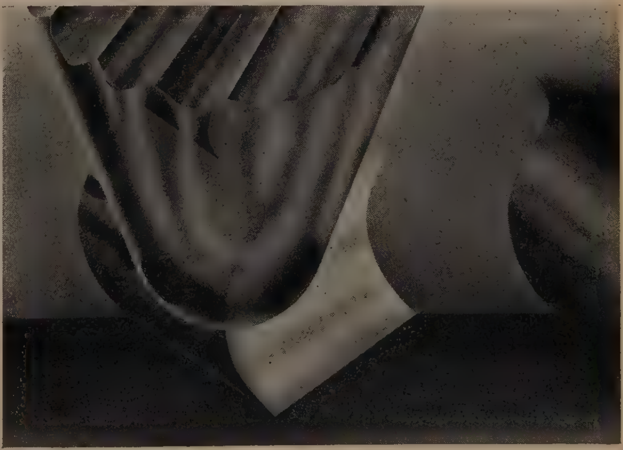

Fig. 4. Perspective drawing, showing the static situation with the stylus resting in a modulated groove.

---

[9] Values in M.K.S. units. The newton is the force necessary to produce an acceleration of 1m/sec$^2$ in a mass of 1 kg, i.e. the force exerted by the weight of $1/g$ kg, where $g = 9.81$ m/sec$^2$; this gives 1 N $\approx$ 1/10 kg weight. Hence to convert the values given to kg/mm$^2$ they should be multiplied by $10^{-7}$.

[10] See Philips tech. Rev. 17, 108, 1955/56 (No. 4).

amplitude will be noted; this will be termed the *static tracing loss*. The amplitude $\hat{\delta}_s$ of this loss is $\hat{y}-\hat{y}_s$.

As long as the record is stationary we are only concerned with a constant vertical force due to the stylus pressure, which can be resolved into two components normal to the groove walls. Although these components are equal in magnitude, it is owing to the opposite curvatures of the walls that they cause impressions of different shapes ($O_1$ and $O_2$ in fig. 5*b*). When the record is turning, additional lateral forces come into play. Let us assume that a sinusoidal signal of constant wavelength is recorded and that the record is now slowly started and gradually speeded up. According to equation (1) the frequency will then gradually increase. As long as the frequency is low, the stiffness force $F_s$ will exceed the inertia force $F_m$ and, apart from the earlier mentioned tracing loss, a *dynamic tracing loss* $\delta_d$ will occur. The total tracing loss $\delta_t$ is the sum of $\delta_d$ and $\delta_s$.

As the frequency becomes higher, $F_m$ increases until at a certain frequency $F_m$ is just equal to the force $F_s$ provided by the stiffness: no external lateral force is then exerted on the stylus. Hence $\delta_d$ becomes zero; the total loss is then equal to the static tracing loss. The frequency at which this happens is called the resonance frequency of the pick-up system. Since the external lateral force on the stylus is now zero, this resonance of the effective mass at the stylus tip and the stiffness of the pick-up system is the same as would occur with the stylus freely vibrating in air, outside a groove.

From $F_m = F_s$, the free resonant frequency is given (see eq. 2) by $s\hat{y}_a = m\omega^2\hat{y}_a$, or $\omega = \sqrt{s/m}$. This resonance does not appear in the actual pick-up characteristic; it occurs, for most pick-ups, at a frequency between about 1000 and 2000 c/s, which is considerably below the *stylus-groove* resonance (to be dealt with later) which has the major effect on the actual characteristic.

At frequencies above the resonance frequency of the pick-up system the force $F_m$ will predominate and the dynamic tracing loss $\delta_d$ will thus become negative, i.e. the total tracing loss will be less than the static loss. At a sufficiently high $F_m$ (hence high frequency and/or large mass) the total loss

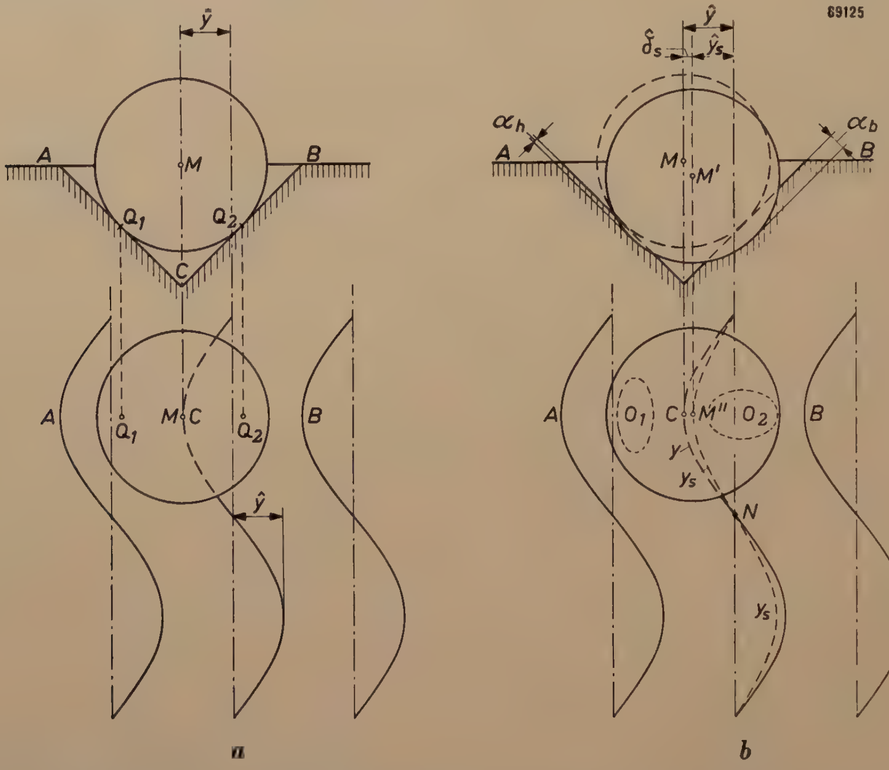

Fig. 5. *a*) Stylus in groove with perfectly rigid walls. Stylus and groove touch at only two points, $Q_1$ and $Q_2$; no horizontal displacement of the centre $M$ of the stylus tip.
*b*) Same for a groove with elastic walls. The points of contact of stylus and groove have now become areas ($O_1$ and $O_2$ shown exaggerated for clarity); the penetration $a_b$ at the convex side of the groove ($B$) is deeper than $a_h$, and consequently $M$ is shifted to $M'$ over a distance whose horizontal projection $CM''$ is $\hat{\delta}_s = \hat{y}-\hat{y}_s$ in the event that the stylus is situated at the crest of the sine. Instead of the recorded sine curve $y$, the stylus describes the curve $y_s$ of smaller amplitude.

may even become negative, and there will therefore be some amplification of the signal. The amplification is greatest at the frequency at which the stylus-groove resonance (stylus-tip inertia and groove-wall stiffness) takes place. This resonance depends on the material of record and stylus, on the shape of groove and stylus and further on the vertical force.

Summarizing, we find that when an ordinary record (unlike our theoretical model modulated with varying wavelength) is played back two opposite effects occur: at higher frequencies the radii of curvature are smaller and therefore the static loss is large, while at the same time the inertia forces increases and thus the dynamic loss is reduced. (This is directly apparent from the signs in (6)). Which of the two effects is predominant depends upon several factors and will be discussed at the conclusion of this article, after dealing with each effect separately.

### Static tracing loss and cut-off frequency

The static tracing loss was defined in the foregoing by $\delta_s = y - y_s$, where $y$ represents the signal registered in the record and $y_s$ the lateral deflection of the stylus tip. The static tracing loss increases according as the radius of curvature of the groove walls becomes smaller. At a given radius (and when the amplitude $\ll$ radius of stylus point, as it always is for the frequencies under consideration), the loss can even equal the original signal: $y = \delta_s$. Then $y_s = 0$; in other words, the stylus describes an unmodulated trajectory and the pick-up does not produce any voltage. We shall evaluate this case for the peak of a sine wave; at this point the deformation is largest and the calculation is simplest.

The following relation exists between the absolute value $|\varrho|$ of the radius of curvature at the peaks and the wavelength or frequency:

$$|\varrho| = \frac{V_g{}^2\sqrt{2}}{\hat{y}\omega^2} = \frac{\lambda^2\sqrt{2}}{4\pi^2\hat{y}} \quad . \quad . \quad . \quad . \quad . \quad (7)$$

where $V_g$ is the velocity of the stylus relative to the unmodulated groove.

The general expression for the radius of curvature of a curve, in Cartesian coordinates, is

$$\varrho = \frac{\left\{1 + \left(\frac{\mathrm{d}y}{\mathrm{d}x}\right)^2\right\}^{\frac{3}{2}}}{\frac{\mathrm{d}^2y}{\mathrm{d}x^2}} .$$

In the present problem, the $x$ coordinate is the direction of the unmodulated groove and the y coordinate is the displacement of the stylus from this axis. At a wave peak $\mathrm{d}y/\mathrm{d}x = 0$, hence

$$\varrho = \frac{1}{\mathrm{d}^2y/\mathrm{d}x^2} .$$

Since $y = \hat{y} \sin \omega t = \hat{y} \sin (\omega x/V_g)$, we have, at the peaks, $\mathrm{d}^2y/\mathrm{d}x^2 = -\hat{y}\omega^2/V_g{}^2 = -4\pi^2\hat{y}/\lambda^2$. The factor $\sqrt{2}$ is introduced in (7) because the radius of curvature considered is in a plane at an angle of 45° with the horizontal plane.

The frequency and wavelength corresponding to the radius of curvature at which the stylus no longer moves laterally, and at which the loss is therefore just as large as the original signal recorded, are called the *cut-off frequency* and the *cut-off wavelength*. At the cut-off frequency, $F_l$ is zero, since the lateral deflection is zero (cf. eq. (3)). However, we shall assume here that $F_l$ is zero throughout the whole frequency range in order to distinguish the static tracing loss from phenomena due to the action of an additional lateral force associated with the dynamic tracing loss. The formulae (6) for the penetration can then be expressed in the following simplified form:

Convex side: $\quad a_b = a_0 \left(1 + \frac{R}{2\varrho}\right)^{\frac{1}{3}}$,

Concave side: $\quad a_h = a_0 \left(1 - \frac{R}{2\varrho}\right)^{\frac{1}{3}}$.

Now, by geometry,

$$\hat{\delta}_s = \frac{a_b - a_h}{2} .$$

Expanding the above expressions for $a_b$ and $a_h$ (neglecting higher powers of $R/2\varrho$) and substituting we get

$$\hat{\delta}_s \approx \frac{a_0}{\sqrt{2}} \times \frac{2}{3}\,\frac{R}{2\varrho} .$$

Using (7) this becomes

$$\hat{\delta}_s = \frac{a_0 R}{6 V_g{}^2}\,\omega^2 \hat{y} .$$

Hence

$$\hat{y}_s = \hat{y} - \hat{\delta}_s = \hat{y}\left(1 - \frac{a_0 R}{6 V_g{}^2}\,\omega^2\right) . \quad . \quad (8)$$

The cut-off frequency $f_{co} = \omega_{co}/2\pi$ and the cut-off wavelength $\lambda_{co}$ are the values at which $\hat{y}_s$ is zero, and hence

$$\omega_{co} = V_g \sqrt{\frac{6}{a_0 R}} \text{ and } \lambda_{co} = \frac{2\pi V_g}{\omega_{co}} = 2\pi \sqrt{\frac{a_0 R}{6}} . \quad (9)$$

We now obtain for $\hat{y}_s$ the following quadratic expressions in terms of $\omega/\omega_{co}$ and of $\lambda_{co}/\lambda$:

$$\hat{y}_s = \hat{y}\left\{1 - \left(\frac{\omega}{\omega_{co}}\right)^2\right\} = \hat{y}\left\{1 - \left(\frac{\lambda_{co}}{\lambda}\right)^2\right\} . \quad . \quad . \quad (10)$$

The former expression is plotted in *fig. 6* (on logarithmic scale).

Since $\omega$ and $\omega_{\text{co}}$ are equally dependent upon the groove velocity $V_g$ (equ. (1) and (9)), the effect of this velocity is not expressed in fig. 6. The fact that this effect is considerable can be readily demonstrated with the aid of a numerical example. Let us assume that $F_v = 0.1$ N ($\approx$ 10 grams), $E = 3.3 \times 10^9$ N/m², $\sigma = 0.35$ and $R = 25 \times 10^{-6}$ m; we then find from (6): $a_0 = 2 \times 10^{-6}$ m. The cut-off wavelength is then $\lambda_{\text{co}} = 2\pi\sqrt{a_0R/6} = 18\mu$, and hence the cut-off frequency is

$$f_{\text{co}} = V_g/\lambda_{\text{co}} = 55\,000\ V_g \text{ c/s}, \quad . \quad . \quad (11)$$

$V_g$ being expressed in metres per second. On the outside of a $33^1/_3$ r.p.m. 12″ record, $V_g = 0.50$ m/s and $f_{\text{co}}$ is consequently 27 500 c/s; on the inside, however, $V_g = 0.20$ m/s and $f_{\text{co}}$ therefore only 11 000 c/s. Under such conditions, therefore, reproduction above 11 000 c/s is impossible near the end of the record, and considerable attenuation occurs even below 11 000 c/s. (This attenuation is more or less compensated when the dynamic tracing loss becomes negative, but it is impossible to profit by this effect above the cut-off frequency).

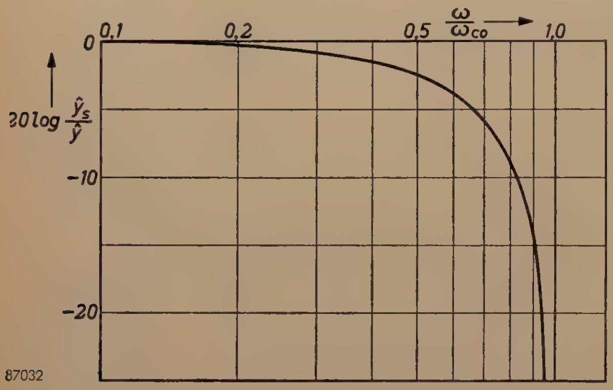

Fig. 6. The ratio $\hat{y}_s/\hat{y} = 1 - (\omega/\omega_{\text{co}})^2$ as a function of $\omega/\omega_{\text{co}}$ (static characteristic, cf. fig. 10); both are plotted on logarithmic scales.

In *fig.* 7, 20 log $\hat{y}_s/\hat{y}$ is plotted as a function of the groove velocity of a $33^1/_3$ r.p.m. record under the above-mentioned conditions, for various frequencies (eq. 8). It can be seen that the reproduction of the high notes is decidedly poorer on the inside than on the outside of the record.

## Dynamic pick-up characteristic, dynamic tracing loss and resonance frequency

The dynamic pick-up characteristic is the characteristic after elimination of the static tracing loss dealt with in the foregoing (thus *including* the dynamic tracing loss).

The dynamic pick-up characteristic can be derived in a simple way by means of an electromechanical analogy [11]). *Fig. 8a* is the equivalent diagram of the mechanical system. The signal $\hat{y} \sin \omega t$ is transferred via the elastic groove wall of stiffness $S$ to the effective mass $m$ concentrated in the stylus tip, the deflection $y_{\text{d}}$ (suffix $_{\text{d}}$ for dynamic) of which we wish to find. The stiffness and the damping of the pick-up are denoted by $s$ and $r$ respectively.

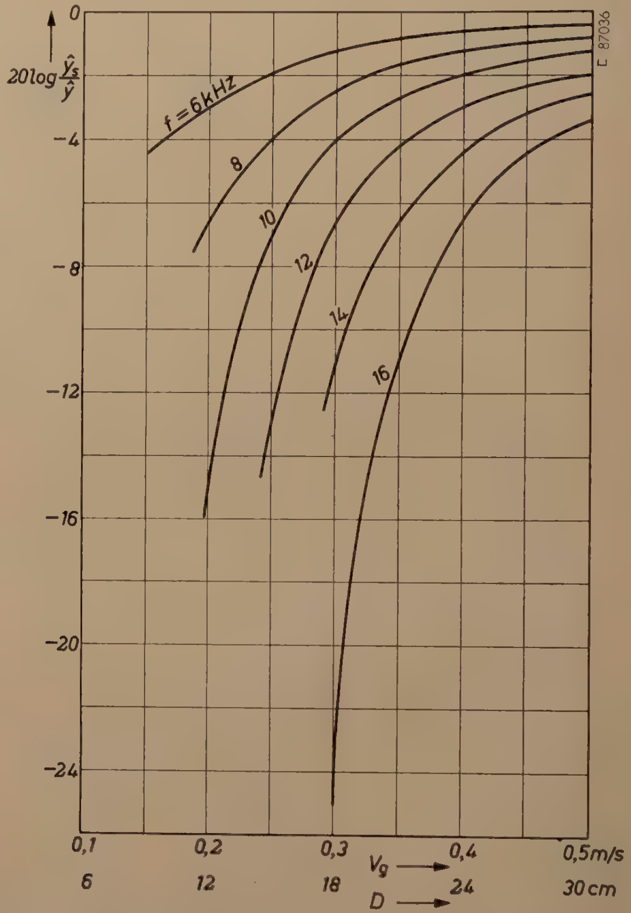

Fig. 7. $\hat{y}_s/\hat{y}$ plotted logarithmically as a function of the groove velocity $V_g$, for a $33\,^1/_3$ r.p.m. record, for various frequencies $f$. For a given r.p.m., $V_g$ is proportional to the distance of the groove from the axis of rotation, i.e. to the groove diameter $D$. The ordinate is therefore also expressed in terms of $D$.

The electrical analogue of this system is shown in fig. 8*b*. The motion of the stylus tip can easily be evaluated from this diagram. We find:

$$\hat{y}_{\text{d}} = \frac{\hat{y}}{\sqrt{\left(1 + \dfrac{s - m\omega^2}{S}\right)^2 + \left(\dfrac{\omega r}{S}\right)^2}} . \quad . \quad (12)$$

---

[11]) For the explanation and the application of electro-mechanical analogies, reference is made to the exhaustive literature on this subject, of which we particularly recommend: B. Gehlshøj, Electro-mechanical and electro-acoustical analogies, Ingenørvidenskabelige Skrifter (no. 1), Akad. tekn. Videnskaber, Copenhagen 1947.

By introducing the natural angular frequency of the stylus-groove system we obtain:

$$\omega_0^2 = \frac{S+s}{m}. \qquad (13)$$

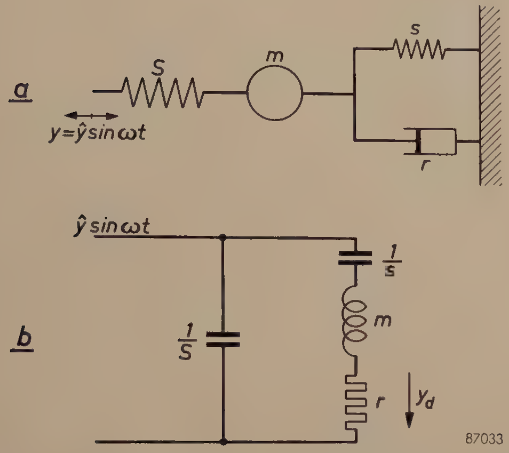

Fig. 8. *a*) Model of the pick-up mechanical system. *m* effective mass and *s* stiffness at the stylus tip, *r* damping, *S* stiffness of the groove wall. $y_d$ is the displacement of the stylus tip resulting from an input signal *y*. *b*) Electrical analogue of (*a*).

Remembering that *s* is many times smaller than *S* [12], so that $\omega_0^2 \approx S/m$, and defining the relative damping coefficient as

$$\varepsilon = \frac{r}{m\omega_0},$$

we can finally put:

$$\hat{y}_d = \frac{\hat{y}}{\sqrt{\left\{1-\left(\frac{\omega}{\omega_0}\right)^2\right\}^2 + \varepsilon^2\left(\frac{\omega}{\omega_0}\right)^2}}. \qquad (14)$$

This formula represents the dynamic pick-up characteristic. The variation of $\hat{y}_d$ as a function of the frequency for various values of the damping is shown in *fig. 9*.

The frequency at which $\hat{y}_d$ assumes the maximum value is the *stylus-groove resonance frequency* $f_{res} = \omega_{res}/2\pi$. By putting $d\hat{y}_d/d\omega = 0$, we find

$$\omega_{res}^2 = \omega_0^2\,(1-\tfrac{1}{2}\varepsilon^2) = \omega_0^2 - \frac{r^2}{2m^2}.$$

The fact that the resonance frequency is lower than the natural frequency is due to the presence of damping; if the damping is small, however, the difference is negligible.

In the foregoing we have introduced the stiffness *S* of the groove walls. The value of *S* can be easily related to $F_v$ and $a_0$ if we take a simplified case [13]). If the stylus rode in an unmodulated groove and was driven by an external lateral force $F_l$, the depths of penetration would be given by a simplified form of (6) since $\varrho = \infty$, i.e:

$$a_{b,h} = a_0\left(1 \mp \frac{F_l}{F_v}\right)^{\frac{2}{3}}.$$

The difference between the recorded and the traced signal, $y - y_d$ is what we have called in the foregoing the dynamic tracing loss $\delta_d$; $y_d = y - \delta_d$ is just a simplified expression of (12). The magnitude of the loss $\delta_d$ is given by expanding the above expressions for $a_b$ and $a_h$ (neglecting higher powers of $F_l/F_v$), subtracting and dividing by $\sqrt{2}$:

$$\delta_d = \frac{a_b - a_h}{\sqrt{2}} \approx \frac{a_0}{\sqrt{2}} \times \frac{4}{3}\,\frac{F_l}{F_v}.$$

The groove wall stiffness *S* is defined as the ratio of the force $F_l$ to the deflection $\delta_d$ due to that force in the presence of the vertical force $F_v$. Hence

$$S = \frac{F_l}{\delta_d} = \frac{F_l}{\frac{a_0}{\sqrt{2}}\,\frac{4}{3}\,\frac{F_l}{F_v}} = \frac{3}{2}\,\frac{F_v}{a_0}\sqrt{2}. \qquad (15)$$

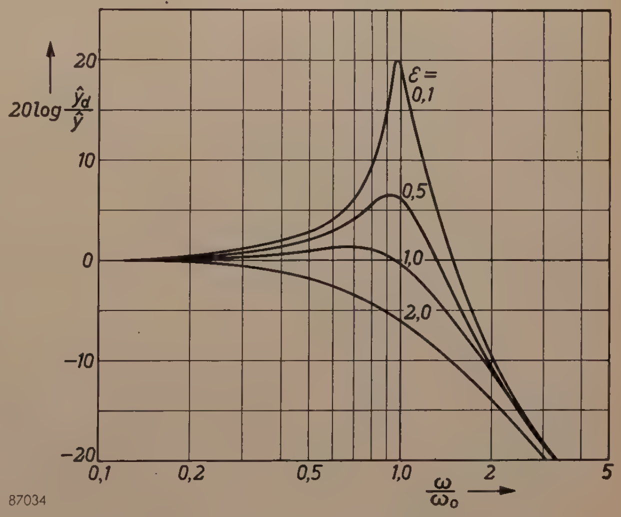

Fig. 9. Dynamic pick-up characteristic $\hat{y}_d = f(\omega/\omega_0)$, for various values of the relative damping coefficient $\varepsilon$ (see eq. (14)). Provided that $\varepsilon$ is not too large a peak occurs at a frequency (the stylus-groove resonance frequency) which lies further below the stylus-groove natural frequency $\omega_0/2\pi$ the stronger the damping. Both scales are logarithmic.

### The actual pick-up characteristic

The actual pick-up characteristic gives the *actual* stylus trajectory $\hat{y}_a$ as a function of the frequency. It consists of a combination of the dynamic pick-up characteristic and the static tracing loss.

---

[12] For ordinary pick-ups, $s$ = 0.02 to 1 kN/m, and for the groove wall $S$ = 40 to 80 kN/m (depending on the material used, on the vertical force $F_v$ and on the radius $R$ of the stylus tip).

[13] It can be shown mathematically that the result obtained here is equivalent to that obtained when the actual conditions are taken into account.

The equation of the actual characteristic can be derived as follows. Consider once again the expression (14) for the dynamic characteristic, keeping in mind that the static loss should, in fact, also be taken into account, so that in (14) $\hat{y}$ should be replaced by $\hat{y}_s$, i.e.

$$\hat{y}_a = \frac{\hat{y}_s}{\hat{y}} \cdot \hat{y}_d .$$

Dividing this by $\hat{y}$ and taking logarithms, we obtain:

$$\log \frac{\hat{y}_a}{\hat{y}} = \log \frac{\hat{y}_s}{\hat{y}} + \log \frac{\hat{y}_d}{\hat{y}} . \quad . \quad . \quad . \quad (16)$$

Hence if the static and the dynamic characteristics are plotted logarithmically on the same frequency scale, we obtain, as is evident from (16), the actual characteristic by adding the two functions. Alternatively, using the expression $y_d = y - \delta_d$, we can obtain the actual characteristic in an analogous manner by substituting in it $y - \delta_s$ for $y$. The result is then:

$$y_a = y - \delta_s - \delta_d = y - (\delta_s + \delta_d) = y - \delta_t ,$$

where $\delta_t$ is the total loss.

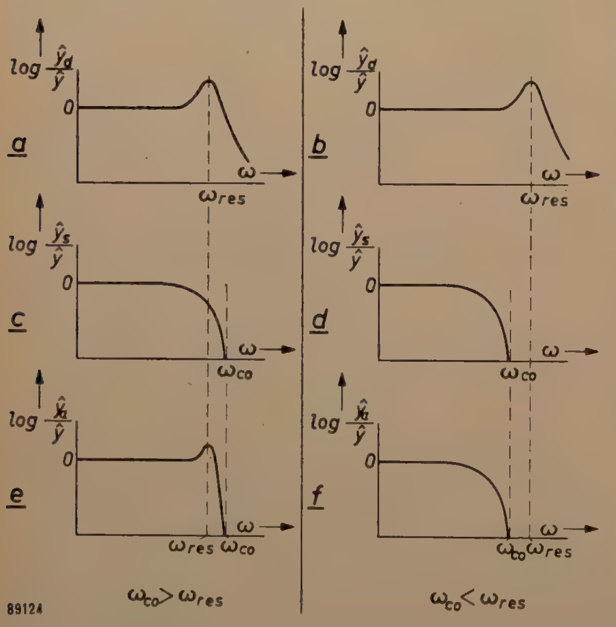

Fig. 10. (*a*) and (*b*) dynamic characteristic $\log \hat{y}_d/\hat{y}$, (*c*) and (*d*) static characteristic $\log \hat{y}_s/\hat{y}$, and (*e*) and (*f*) actual characteristics $\log \hat{y}_a/\hat{y} = \log \hat{y}_d/\hat{y} + \log \hat{y}_s/\hat{y}$; (*a*), (*c*) and (*e*) refer to $\omega_{co} > \omega_{res}$; (*b*), (*d*) and (*f*) refer to $\omega_{co} < \omega_{res}$.

Log $\hat{y}_d/\hat{y}$, log $\hat{y}_s/\hat{y}$ and their sum log $\hat{y}_a/\hat{y}$, are plotted in *fig. 10*, on the left for the case of $\omega_{co} > \omega_{res}$, and on the right for $\omega_{co} < \omega_{res}$.

In the former case the drop due to the static loss below the resonance frequency is reduced by the resonance peak in $\hat{y}_d$; there remains a resonance peak in $\hat{y}_a$, although less pronounced than in $\hat{y}_d$, whilst the in region beyond the resonance frequency the cut-off is now sharper. In the second case ($\omega_{co} < \omega_{res}$) the actual characteristic is virtually identical with the static one.

### The practical importance of the various properties of pick-up and record

Consider the resonant angular frequency $\omega_0$ of the stylus-groove system and the cut-off wavelength $\lambda_0$. For the former quantity we take (13) in the approximate form $\omega_0^2 \approx S/m$, substitute for $S$ from (15) and then insert the value of $a_0$ defined by equation (6). For $\lambda_{co}$, we simply insert the value of $a_0$ from (6) in equation (9). We then obtain:

$$\omega_0 = \left\{ \frac{6}{\sqrt{2}} \frac{F_v R}{m^3} \frac{E^2}{(1-\sigma^2)^2} \right\}^{\frac{1}{6}} , \quad . \quad . \quad . \quad (17a)$$

$$\lambda_{co} = \left\{ \frac{\pi^3}{\sqrt{12}} F_v R \frac{1-\sigma^2}{E} \right\}^{\frac{1}{3}} . \quad . \quad . \quad . \quad . \quad (17b)$$

$\omega_0$ and $\lambda_{co}$ are quantities dependent only on the physical properties of the pick-up, the properties of the record material, and the vertical force $F_v$. They are therefore independent of the groove velocity and of the amplitude of the signal. For a given pick-up and a given record, $\omega_0$ and $\lambda_{co}$ are to be regarded as system constants, which can be varied only by changing $F_v$. The cut-off frequency, however, as we have shown earlier, is determined by the relation $\omega_{co} = 2\pi V_g/\lambda_{co}$ and is consequently directly proportional to the groove velocity: $\omega_{co}$ will thus be higher on the outside than on the inside of the record. The position of the stylus on the record will therefore be one of the factors deciding whether $\omega_{co}$ is greater or smaller than $\omega_{res}$ (in most cases $\omega_{res}$ is virtually equal to $\omega_0$). From the above the following conclusions may be drawn:

1) A reduction of the effective mass $m$ at the stylus tip has no effect on $\lambda_{co}$ but it does raise the natural frequency $\omega_0$ and consequently improves the reproduction of the high notes, provided that $\omega_0 < \omega_{co}$.
2) The stiffness of the pick-up does not appear in (17*a* or *b*) and therefore affects neither $\lambda_{co}$ nor $\omega_0$. This is valid only for the high frequencies discussed here; $s$ is obviously of importance at the lower frequencies.
3) The damping $r$ of the pick-up determines the height of the resonance peak; it does so, however, in conjunction with the damping of the record material. The latter factor does not appear in the above considerations owing to the simplification introduced.

4) Increasing the Young's modulus $E$ of the record material produces an increase in $\omega_0$ and a reduction of $\lambda_{co}$. As mentioned in connection with the groove deformation, a shellac record, whose Young's modulus is about twice that of a plastic record, will be more favourable in this respect. Owing to other factors, however, such as the reduced noise and the unbreakability, the plastic material is nevertheless to be preferred (cf. the articles quoted in 6) and 10)).

5) The radius of curvature $R$ of the stylus tip is 25 μ for long-playing records and 75 μ for normal (78 r.p.m.) records. This greater radius causes a higher $\omega_0$ but also a greater $\lambda_{co}$ and, therefore, a greater static tracing loss if the same record material is used. Normal records, however, are usually made of shellac, which, as mentioned in 4) above, has a greater Young's modulus than plastic, and this partly compensates for the greater loss due to the greater radius of curvature of the stylus tip. According to (17*b*) $\lambda_{co}$ is proportional to $(R/E)^{\frac{1}{3}}$, so that the cut-off wavelength $\lambda_{co}$ for shellac ($R = 75$ μ, $E = 6 \times 10^9$ N/m²) will be a factor of

$$\left(\frac{75}{25} \times \frac{3.3}{6}\right)^{\frac{1}{3}} = 1.18$$

greater than for co-polymer plastic ($R = 25$ μ, $E = 3.3 \times 10^9$ N/m²). On the smallest diameter (9.5 cm) of a 78 r.p.m. record the groove velocity $V_g$ is approx 1.85 times greater than on the smallest diameter (12.5 cm) of a 33⅓ r.p.m. record, so that according to equation (1) the cut-off frequency in the former case will be higher by a factor of 1.85/1.18 ≈ 1.6 than in the latter case.

6) The vertical force $F_V$, to which the styles pressure is proportional, also affects $\omega_0$ and $\lambda_{co}$ as shown by (17): a reduction of the stylus pressure reduces $\lambda_{co}$ and together with it the tracing loss, but $\omega_0$ is then also reduced.

In a later article it will be shown how the above considerations have been applied in the design of a new pick-up.

**Summary.** As an introduction to an article on a new gramophone pick-up the mechanics of the system pick-up — gramophone record are considered. The stylus (sapphire, diamond) whose spherical tip rides in the groove of the record, causes elastic deformation of the groove walls. The convex wall is deformed to a greater depth than the concave wall. This causes a loss in the stylus deflection, the static tracing loss. This loss is greater the smaller the radius of curvature of the groove, i.e. the higher the frequency, the larger the amplitude and the nearer the stylus is to the centre of the disc. At a given frequency — the cut-off frequency — this loss is equal to the recorded signal, so that the stylus tip does not vibrate at all; this loss becomes apparent even considerably below the cut-off frequency.

A second effect — the dynamic tracing loss — has likewise the nature of a loss as long as the stiffness force of the pick-up exceeds the inertia force on the stylus tip; this is the case at frequencies below the free resonance frequency of the pick-up system. At higher frequencies this loss becomes negative and thus acts in opposition to the static loss. The total loss (the sum of the static and the dynamic losses) may even become negative. This is liable to happen particularly in the neighbourhood of the frequency at which resonance of the groove-wall stiffness and the effective mass at the stylus tip occurs; the resonance curve of this system is called the dynamic pick-up characteristic. A combination of the latter with the static characteristic produces the actual pick-up characteristic. According to whether the cut-off frequency lies higher or lower than the stylus-groove resonance frequency, the actual characteristic will either show a slight peak or no peak at all. The article is concluded with a discussion of the practical significance of the various properties of pick-up and record.

---

# ABSTRACTS OF RECENT SCIENTIFIC PUBLICATIONS BY THE STAFF OF N.V. PHILIPS' GLOEILAMPENFABRIEKEN

Reprints of these papers not marked with an asterisk * can be obtained free of charge upon application to Philips Electrical Ltd., Century House, Shaftesbury Avenue, London W.C. 2.

**2296:** P. W. L. Iterson and H. A. Teunissen: General outline of the development of transmitters for television and frequency modulation (T. Ned. Radiogenootschap **20**, 207-222, 1955, No. 3).

Description of some TV and FM transmitters together with their auxiliary equipment developed in recent years by Philips Telecommunications Industries. Some details are given of design and properties. Special features are the use of high power tetrodes, a special FM modulation circuit and unit construction which lead to simple installations of high performance. An FM transmitter is described which works without supervision and switches over automatically to reserve equipment in the event of a failure.

**2297:** H. O. Huisman, R. van der Veen and J. Meltzer: A new acaricide, 2,4,5,4′-tetrachlorodiphenylsulphone (Nature **176**, 515-516, 10 September 1955).

Note on the action of the above-mentioned acaricide. It acts on the eggs and larvae of a number of mites but is ineffective against the fully-grown animals. The action is very selective: only mites are sensitive. Insects show no reaction and the acaricide is not poisonous to mammals.

**2298:** H. Groendijk and K. S. Knol: Characterization of the noise of tubes and transistors by four measurable quantities (T. Ned. Radiogenootschap **20**, 243-256, 1955, No. 4).

The noise of a neutralized triode is first calculated by investigating the mechanism of noise production and then by regarding the triode as a linear four-terminal network. It appears, from the first method, that the physical quantities connected with the generation of noise may not readily be determined. The second method shows, however, that it is still possible to characterize the noise by four measurable quantities and, once these are known, to calculate the noise factor. This holds for any linear four-terminal network, triodes, pentodes, transistors, etc. In general, no simple relationship exists between these quantities and the physical properties giving rise to noise. In the case of a triode the four quantities depend on frequency in a simple way. See also these abstracts No. **R 277**.

**2299:** J. A. Lely: Darstellung von Einkristallen von Siliciumcarbid und Beherrschung von Art und Menge der eingebauten Verunreinigungen (Ber. Deutsch. Keram. Gesellsch. **32**, 229-231, 1955, No. 8). (Preparation of single crystals of silicon carbide and control of type and quantity of lattice impurities; in German).

See these abstracts No. **2267.**

**2300:** A. C. van Dorsten and J. H. Spaa: Een hoogspanningsgenerator in druktank voor neutronenproduktie (Ned. T. Natuurk. **21**, 213-218, 1955, No. 9). (A pressurized high-voltage generator for neutron production; in Dutch).

Short description of equipment for producing a neutron flux of $10^{10}$ fast neutrons per second by the bombardment of a heavy ice target with deuterons. See Philips tech. Rev. **17**, 109-111, 1955/56.

**2301:** B. Combée, J. Houtman and A. Recourt: A sealed-off X-ray tube for contact-microradiography (Brit. J. Radiol. **28**, 537-542, October 1955).

Short description of a new sealed-off X-ray tube for contact microradiography using a 50 μ Be window (see also Philips tech. Rev. **17**, 45-46, 1955/56). Calculations and measurements are given concerning the properties of photographic emulsions in the interesting range of wavelengths between 2-12 Å.

**2302:** M. Gevers: Measurement of dielectric and magnetic properties of solids at microwave frequencies (Proc. Symposium Precision Electrical Measurements, National Physical Laboratory, Teddington, Nov. 1954).

Description of two of the methods used for measuring dielectric and magnetic properties of solids at cm wavelengths in the Philips Research Laboratories, Eindhoven. At 10 cm a resonance method is used and at 3 cm a method based on standing waves. Special attention is paid to the sources of errors and the accuracy of the measurements on low loss materials.

**2303:** J. W. L. Köhler: Machines frigorifiques à gaz froid (Annexe 1955-2, Suppl. Bull. Inst. Int. Froid, pp. 13-23).

See Philips tech. Rev. **16**, 69-78 and 105-115, 1954/55. Special attention is paid in this article to the properties of the regenerator which include one condition not hitherto recognized.

**2304:** J. Volger: Pertes dielectriques de quelques verres et de substances similaires, mesurée aux basses températures (Annexe 1955-2, Suppl. Bull. Inst. Int. Froid, pp. 89-98).

The dielectric losses of quartz and various silicate glasses have been studied at low frequencies. Round about 50 °K a new type of loss — so-called deformation loss — appears. The relation between these phenomena and the glass structure is discussed.

**2305:** G. Diemer: Transit-time functions of a dynatron oscillator (Appl. sci. Res. **B 4**, 457-463, 1955).

The transit-time functions of the dynode admittance are discussed for a new type of dynatron-oscillator, in which the primary electrons are directed obliquely towards the dynode.

**2306:** J. A. Kok and M. M. G. Corbey: Breakdown of liquid insulating and dielectric material (Appl. sci. Res. **B 4**, 474-475, No. 6).

Preliminary note on experiments and theory of long-term breakdown of liquid dielectrics at low frequencies.

**2307:** J. Meltzer: Het onderzoek van acariciden en spintoviciden in het laboratorium (Tijdschrift Plantenziekten **61**, 130-142, 1955). (The investigation of acaricides and red spider ovicides in the laboratory; in Dutch, summary in English).

Description of laboratory methods for the evaluation of acaricidal and ovicidal action of a large number of substances. The substances concerned fall into three groups: those active an adult mites, those active on eggs and immature mobile stages and those active on all three stages. The results are summarized in 13 tables.

**2308:** L. J. Tummers: Der Einfluss von Minoritätsträger-Injektionen auf das Verhalten von Leistungstransistoren (Nachr.-techn. Fachber., 1955, No. 1, pp. 31-32). (The effect of minority carrier injection on the behaviour of power transistors; in German).

The emitter efficiency of a p-n-p alloy transistor with indium as the alloying material can be increased by adding a small amount of gallium or aluminium to the emitter indium. This improved emitter efficiency causes a more gradual fall off of the current amplification at increasing emitter currents and furthermore makes it possible to produce transistors with lower base resistance.

**2309:** J. C. van Vessem and Th. W. Willemse: Konstruktive Überlegungen beim Entwurf eines Leistungstransistors (Nachr. techn. Fachber. 33-36, 1955, No. 1). (Design considerations concerning power transistors; in German).

Design of a power transistor for a dissipation of 3 watts and description of the considerations which lead to this design.

**2310:** P. F. Moleman: Thermische Probleme bei der Verwendung von Schichttransistoren (Nachr. Techn. Fachber. 37-39, 1955, No. 1). (Thermal problems in the application of junction transistors; in German).

Study of the properties of a well-known circuit for the temperature stabilization of a transistor. When this circuit is used in a push-pull arrangement it is necessary to take account of the effect of temperature not only on the collector leakage current but also on the emitter-base potential difference.

**2311:** G. H. Jonker and H. R. Kruyt: Flocculation and recrystallization in freshly prepared silver bromide sols (Discussions Faraday Soc. No. 18, 170-190, 1954).

The ageing of diluted silver bromide sols has been studied by extinction measurements. The sols initially contain very small particles which flocculate to a certain degree, depending on the excess concentration of $Ag^+$ or $Br^-$ ions. In very diluted sols a new type of coarsening is found in the region of normally stable negative sols. By studying the influence of electrolytes, protecting colloids and temperature it is found that this new type of coarsening consists of two stages: first a recrystallization takes place to rather large crystals and then still larger particles are formed by oriented flocculation of the ideally formed crystals. The same effect has been found in sols of silver chloride at higher concentrations and in silver iodide at lower concentrations.

**2312:** F. A. Kröger and D. de Nobel: Preparation and properties of CdTe single crystals (J. Electronics 1, 190-202, 1955).

Single crystals of CdTe were prepared and purified using the method described in abstract **2313** (see below). By re-heating below the melting point under suitable atmospheres the stoichiometry and hence the electrical properties were modified. Both *p* and *n* type conductivity have been obtained. Measurements of Hall effect, the thermoelectric power and the resistance give values of the mobility and the effective mass of electrons and holes and an idea of the energies of donor and acceptor levels.

**2313:** J. van der Boomgaard, F. A. Kröger and H. J. Vink: Zone melting of decomposing solids (J. Electronics 1, 212-217, 1955).

Zone melting of substances which tend to decompose on heating can be accomplished by heating in an atmosphere of the component formed on decomposition. By means of the pressure of this component it is possible to control the composition of the crystals obtained from the melt. As an example, the growth of a PbS crystal with a *p-n* junction is described.

**2314:** R. Vermeulen: Stereophonie und Stereonachhall (Musik-Raumgestaltung-Elektroakustik, 1955, Arsvira Verlag, Mainz). (Stereophony and artificial reverberation; in German).

See Philips techn. Rev. 17, 258-266, 1955/1956.

**2315:** H. Koelmans and J. Th. G. Overbeek: Stability and electrophoretic deposition of suspensions in non-aqueous media (Disc. Faraday Soc. 1-12, 1954).

The stability of suspensions in solvents of very low polarity is treated in part 1 of this paper. Theoretical considerations lead to the conclusion, that quite modest electric charges and $\zeta$-potentials are sufficient to stabilize suspensions of coarse particles ($> 1\ \mu$) whereas hardly any stabilization can be expected from adsorbed layers of non-ionized long-chain molecules. Experiments on the settling times of suspensions of a number of solids in xylene confirm that only ionized surface-active substances give rise to stability. Long-chain compounds that do not increase the conductance of the xylene, do not give rise ro a sufficient $\zeta$-potential of the particles and do not improve the stability very much. In part 2 electro-deposition from suspensions in polar organic media is investigated. It is shown that the particles are accumulated near the electrode by the applied field, but that the formation of an adhering deposit is caused by flocculation introduced by the electrolyte formed by the electrode reaction.

**2316:** A. G. Th. Becking, H. Groendijk and K. S. Knol: Kennzeichnung der Rauscheigenschaften von Vierpolen (Nachr. Techn. Fachber. 37-40, 1955). (Characterization of the noise properties of fourpoles; in German).

See abstract **2298** and abstract **R 277.**

**2317:** A. N. Diddens, F. L. H. M. Stumpers and J. Volger: Das Rauschen eines keramischen Halbleiters, dessen Widerstand von der Frequenz und von Magnetfeld abhängig ist (Nachr. Techn. Fachber. 88-89, 1955). (The noise of ceramic semiconductors whose resistance is dependent on frequency and on magnetic field; in German).

The noise voltage of a specimen of the material $La_{0.9}Sr_{0.1}MnO_3$, previously shown to have a frequency and magnetic-field dependent resistance, has been investigated. As expected the thermal noise satisfies the Nyquist formula $\overline{\Delta V^2}/\Delta f = 4kTR(f,H)$, where $R(f,H)$ is the real part of the impedance of the specimen at the frequency $f$ and in the magnetic field $H$. A direct current $i$ increases the noise strongly as in many polycrystalline materials. The spectrum of the current noise is given by $\overline{\Delta V^2}/\Delta f = K(f,H)\, i^{\alpha} f^{-\beta}$ where $\alpha = 1.3$-$1.7$, $\beta = 0.9$ and $K$ is proportional to the value of $R(f,H)$.

**2318:** P. Schagen: The "scenioscope", a new television camera tube (T. Ned. Radiogenootschap **20**, 291-305, 1955).

Description of a new television camera tube based on the use of a target of semi-conducting glass. See Philips tech. Rev. **17**, 189-198, 1955/1956.

**2319:** J. Smit: The spontaneous Hall effect in ferromagnetics, I (Physica **21**, 877-887, 1955).

Apart from the normal Hall voltage a magnetized ferromagnetic material usually shows a relatively large extra voltage in the same direction, which can be found by linear extrapolation to $B = 0$. It is shown that this spontaneous Hall effect cannot exist in a perfectly periodic lattice. Measurements at different temperatures suggest that the effect is closely related with the electrical resistivity of the material. Existing theories on the origin of the effect are shown to be invalid, and it is shown that the explanation has to be based on the anisotropic scattering, caused by spin-orbit interaction of the conducting electrons against the imperfections of the lattice.

**2320:** R. Thoraeus, W. J. Oosterkamp, J. Proper, R. Jaeger, B. Rajewsky, E. Bunde, M. Dorneich, D. Lang and A. Sewkor: Vergleichsmessungen der internationalen "röntgen" im Bereich von 8 kV bis 170 kV Erzeugungsspannung (Strahlentherapie, **18** (2), 1955. (Comparative measurements of the international röntgen for generating voltages from 8 kV to 170 kV; in German).

Joint publication from the Radiofysika Institutionen. Stockholm, the Philips Research Laboratories, Eindhoven, the Physikalisch-technische Bundesanstalt, Braunschweig and the Max Planck-Institut für Biophysik, Frankfurt/Main. The main results are given of a comparison between the standard instruments for measuring hard and soft X-rays of the Max Planck Institut für Biophysik and Swedish and Dutch instruments. The measurements with hard X-rays are in good agreement with each other. The comparisons in the soft X-ray region, where errors are by nature larger, show fairly good agreement; studies are planned to improve measuring instruments and methods in this region in order to reduce the still existing differences.

**2321:** J. W. L. Köhler and J. van der Ster: A small liquid nitrogen plant using a gas refrigerating machine (Proc. 9th Int. Congress Refrigeration, Paris, Sept. 1955).

Description of an installation producing liquid nitrogen on a small scale. A rectifying column is coupled to a gas refrigerating machine supplying the necessary cold. The air to be fractionated is not compressed at all, which makes the installation extremely simple. The single column is of the packed type; the incoming air is utilized to reboil the liquid with the higher boiling point. The vapor, issuing at the top of the column, is condensed by the gas refrigerating machine: the resulting liquid is partly utilised as reflux in the column, the rest forming the product. The completely automatic plant is run fully unattended. Relevant constructional details and results are given.